REVIEW

Chinese Journal of Structural Chemistry

Recent Progresses in Lanthanide Metal-Organic Frameworks (Ln-MOFs) as Chemical Sensors for Ions, Antibiotics and Amino Acids

Yan Yang[1]*, Shuting Xu[1], Yanli Gai[3], Bo Zhang[1] and Lian Chen[2]*

[1]*College of Chemistry and Chemical Engineering, Liaocheng University, Liaocheng 252059, China*
[2]*State Key Laboratory of Structure Chemistry, Fujian Institute of Research on the Structure of Matter, Chinese Academy of Sciences, Fuzhou 350002, China*
[3]*School of Chemistry and Materials Science, Jiangsu Normal University, Xuzhou, Jiangsu 221116, China*

ABSTRACT Various ions and antibiotics, widely used in industry and clinical medicine, respectively, are massively discharged to atmosphere and water, resulting in severe pollutions on environment and potential threats to human health. Besides, amino acids, the primary substances for the establishment of proteins, cells and tissues, are crucial to human health. Therefore, seeking effective and practicable materials to detect aforesaid analytes is vitally meaningful. Metal-organic frameworks centered with lanthanide ions (Ln-MOFs), also known as lanthanide coordination polymers, are considered as a charming category of multi-functional hybrid crystalline materials with fascinating structures and incomparable luminescent characteristics. Benefited from their unique merits, Ln-MOFs have been largely developed as excellent luminescent sensors for fast and efficient sensing various analytes. In this review, we aim to introduce some of the recent researches between 2018 to 2022 on Ln-MOFs applied as chemical sensors for ions, antibiotics and amino acids based on luminescent quenching and enhancing effects, and provide an update and summary for the latest progresses in this field.

Keywords: lanthanide metal-organic frameworks, luminescence, luminescent sensors, sensing mechanism

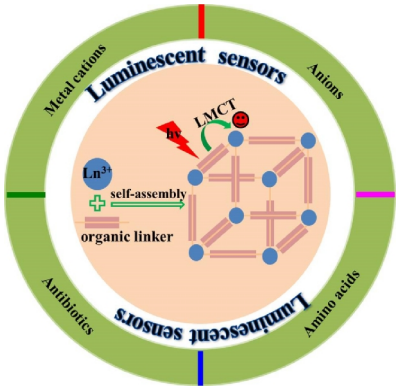

n INTRODUNTION

Metal-organic frameworks (MOFs), a burgeoning class of organic-inorganic hybrid crystalline materials, have exerted a strong momentum of growth in the past decades.[1-7] Self-assembly of various inorganic metal ions/clusters and organic linkers readily generates fascinating MOFs featured with diverse structures, lager porosity and surface areas, variable pore sizes, modifiable pore surface, et al.[8-15] As a special class of MOFs, lanthanide MOFs assembled by Ln^{3+} and organic ligands have more advantages than MOFs centered with transition metal ions, thanks to the unique luminescent properties of lanthanide ions, such as characteristic sharp emissions, high quantum yields, millisecond lifetimes, large Stocks shifts, and so on.[16-19] Besides, Ln^{3+} ions possess high coordination numbers from 6 to 13 and multiple coordination modes. When all lanthanide sites are coordinated with organic ligands, the structures can be stabilized. Thus, Ln-MOFs can be applied as a unique class of luminescent sensors compared with other traditional materials. On one hand, the porous structures of Ln-MOFs may provide more opportunities for host-guest interactions, and then increase the sensitivity of these luminescent sensors. On the other hand, the presence of open lanthanide sites or other functionalized sites, such as Lewis basic sites and Lewis acid sites supplied by organic linkers, is beneficial to forming interactions between these open active sites and various guest substances.[20-22] Besides, lanthanide ions, especially Eu^{3+} and Tb^{3+}, exhibit sharp typical emissions. The luminescent response can be evaluated by monitoring the variations of emission intensities. Moreover, changes of the light colors for most Ln-MOFs can be distinguished by the naked eyes. In virtue of functionalized structures and characteristic luminescence, a great number of Ln-MOFs have been developed and utilized as luminescent chemical sensors for metal ions,[23-32] anions,[33-41] small organic solvent molecules,[42-50] nitro-aromatic explosives,[51-59] temperature,[60-66] antibiotics,[67-72] amino acids[73-75] and biomarkers[76-86], and so forth.

n LUMINESCENCE of Ln-MOFS

For Ln^{3+} ions, the last electrons are successively filled in the 4f orbitals, giving the characteristic electron configuration of Ln^{3+} ions from $[Xe]4f^{0}$ to $[Xe]4f^{14}$, corresponding to La^{3+} ions to Lu^{3+} ions. The shielding effects on the 4f electrons from the outer filled 5s and 5p subshells result in the Laporte forbidden of f-f traditions, giving the long-lived narrow emissions and characteristic colors for Ln^{3+} ions. Due to the Laporte-forbidden transitions, only weak luminescent emissions are observed when Ln^{3+} ions are direct excited.[87-89] Fortunately, this conundrum can be solved by introducing sensitizers, which can transfer the adsorbed energy to Ln^{3+} ions and then induce the strong luminescence of Ln^{3+} ions. Such energy transfer processes, known as “antenna effect”, consist of four steps: light adsorption of the organic ligand, exciting the luminophore from its ground state (S_0) to the singlet excited state (S_1); energy transition from S_1 to the triplet states (T_1) through intersystem crossing process (ISC); intermolecular energy transfer from the T_1 of ligands to the excited states of Ln^{3+} ions; radiative transition of excited Ln^{3+} ion to the ground state, resulting in the luminescence of Ln^{3+} ions (Scheme 1).[90-92] When the energy transfer from the ligand to the centered Ln^{3+} ion is

Chin. J. Struct. Chem. **2022**, 41, 2211045-2211070
DOI: 10.14102/j.cnki.0254-5861.2022-0138

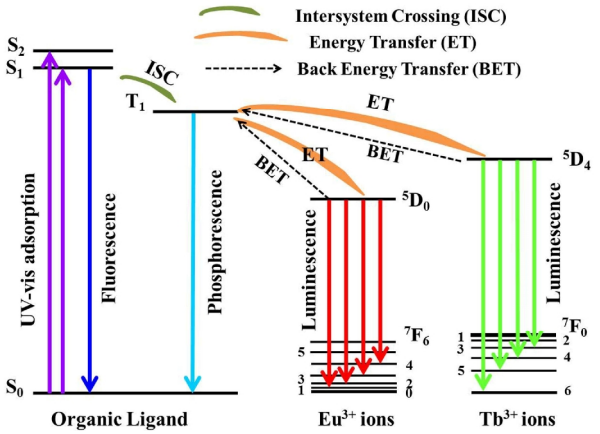

Scheme 1. Schematic of the energy adsorption, transfer and emission processes (S: singlet state; T: triplet state).

thoroughly efficient, the emission of the ligand is completely quenched. If the efficiency of energy transfer is not high enough, the dual emissions of the ligand and Ln^{3+} ion co-exist.

As discussed above, the energy matching between the triplet states T_1 of ligands and the lowest excited states of Ln^{3+} ions plays a vital role in the luminescent properties of Ln-MOFs. The excitation energy will be released through non-radiative transition processes if Ln^{3+} ions are excited to non-emissive levels. The lowest excited states of Eu^{3+} and Tb^{3+} are $^5D_0$ and $^5D_4$ levels, located at 17267 and 20500 cm^{-1}, respectively. According to Latva's empirical rule, for Eu^{3+} and Tb^{3+} ions, the energy gaps ($\Delta E = T_1 - {}^5D_J$) for optimal energy transfer processes from the ligands to Ln^{3+} ions should fall in the ranges of 2500-4000 and 2500-4500 cm^{-1}, respectively. Thermal-activated energy back-transfer process will occur when the energy gap between ligands and Ln^{3+} ions is too small, while too big energy gaps may result in the reduction of energy transfer rates.[93-94] Therefore, selecting ligands with suitable triplet state energies is quite important for the design and synthesis of Ln-MOFs featuring with excellent luminescent performance.

In terms of the unique luminescent properties and diverse structures, the applications of Ln-MOFs on the detection for various harmful substances have been summarized in recent years.[95-102] Herein, we have researched and summarized recent progress in regard to the luminescent sensors based on Ln-MOFs towards ions, antibiotics and amino acids (Table 1 and Table 2).

n Ln-MOFS APPLIED AS LUMINESCENT SENSORS

Sensors for Ions

Sensors for Metal Cations. Metal cations, especially hazardous metal cations, such as Pb(II), Cu(II) and Fe(III), are commonly utilized in industrial manufacture and play an important role in the biological system of human body. However, most metal cations are poisonous and bio-toxic, and can bring about protein denaturation, enzyme inactivation and even carcinogenesis if they are the beyond dangerous threshold.[4,22] For instance, the overdose and deficiency of Fe^{3+} ions may cause a certain degree of lesion to the body function and then result in various diseases, such as liver cirrhosis, cardiac failure, diabetes mellitus and iorn-deficiency anemia.[103-104] Excessive amounts of Cd^{2+} ions in body can cause gastrointestinal dysfunction and bone softening, and even aggravate the burden of liver and kidney owing to the fact of difficult excretion. In addition, long-term exposure to the environment containing Cd^{2+} ions can result in anosmia, gingival spots or yellow rings.[4,105] Therefore, developing effective, convenient and fast-responsive sensors for trace metal cations is extremely important. In recent years, numerous Ln-MOFs are developed and utilized to detect various in trace amounts.[106-112]

Bu et al. employed an aggregation-induced emission (AIE) linker to fabricate a new Tb-MOF (**1**) with super chemical stabilities in various organic solvents and aqueous solutions of pH = 1-14 for Fe^{3+} detection in aqueous solution.[113] Different from other reported Ln-MOFs, compound **1** displayed fluorescence derived from the ligand, rather than Tb^{3+} ions, because the energy gap between the triplet-state energy T_1 of the ligand (20055 cm^{-1}) and the lowest excited states of Tb^{3+} ($^5D_4$: 20500 cm^{-1}) fell outside the energy gaps for efficient "antenna effect" (2500-4500 cm^{-1} for Tb^{3+}). Featuring the outstanding stability and strong emission, **1** exhibited a remarkable response to Fe^{3+} based on luminescent "turn-off" effect with anti-interference ability and renewability, the K_{sv} and detection limit of which were 3.50×10^3 M^{-1} and 138.8 ppm, respectively. The presence of the large

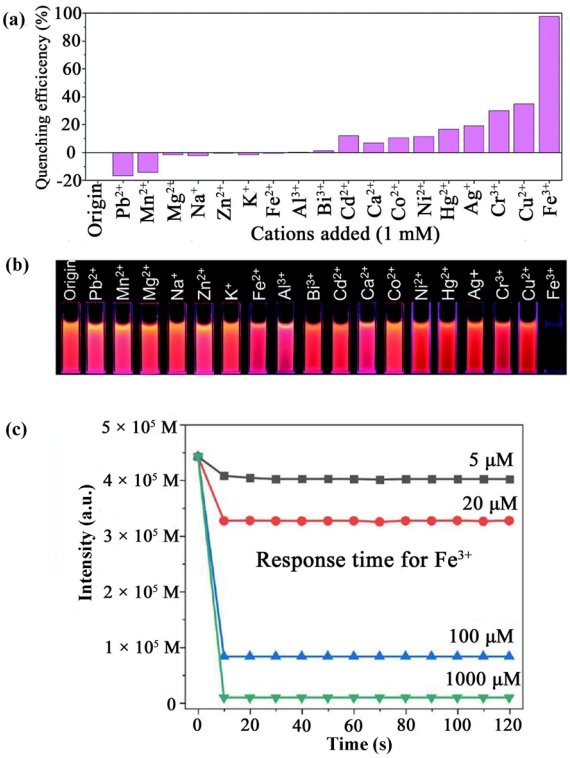

Figure 1. (a) Quenching efficiency of **2** in aqueous solutions containing various cations (1 mM). (b) Photographs of **2** in aqueous solutions containing various cations (1 mM) under 254 nm UV irradiation. (c) Luminescent intensities of **2** at different response time in the presence of Fe^{3+} at different concentrations. Reproduced with permission from Ref.[114]

DOI: 10.14102/j.cnki.0254-5861.2022-0138

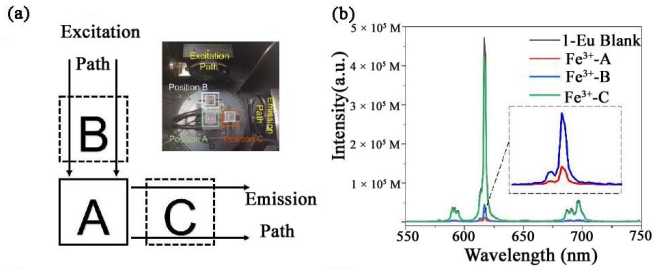

Figure 2. (a) Scheme of the luminescent quenching mechanism experiment. (b) The emission spectra of **2** (excited at 280 nm) with Fe^{3+} (Black curves: **2** solely in position A; red curves: mixture of **2** and Fe^{3+} in position A; blue curves: **2** in position A while Fe^{3+} in position B; green curves: **2** in position A while Fe^{3+} in position C). Reproduced with permission from Ref.[114]

overlap between the UV-*vis* absorption band of Fe^{3+} and the excitation and emission spectra of **1** indicated that the mechanism of luminescent "turn-off" effect for **1** towards Fe^{3+} was the combination of competitive absorption between Fe^{3+} and **1**, and fluorescence resonance energy transfer (FRET).

In another work, a new water-stable Eu-MOF (**2**) with an open 1D channel with the size of 8.9 × 8.9 $Å^2$ was developed by Zang and co-workers.[114] Compound **2** displayed typical red emissions of Eu^{3+} ions. And luminescent sensing measurements revealed that the luminescent intensity of **2** was quenched by Fe^{3+} with the quenching efficiency of 97.7% (Figure 1a). Under 254 nm UV lamp, compared with other analytes, the color of suspension with Fe^{3+} changed from original red to blue, revealing that compound **2** can selectively distinguish Fe^{3+} distinguished by the naked eye (Figure 1b). Further, the fluorescence titration experiments indicated that compound **2** was a potential probe of Fe^{3+} with high sensitivity, giving the limit of detection (LOD) and K_{sv} of 0.57 mM and 3.50 × 10^3 M^{-1}, respectively. Moreover, the exploration of response time was performed, showing the luminescent intensity of **2** gave a fast response just in 10 seconds (Figure 1c). In addition, to explore the quenching mechanism, a series of verified experiments were executed. As shown in Figure 2, when the suspension of **2** and the solution of Fe^{3+} were placed in position A and B, respectively, the luminescent intensity was obviously decreased. Whereas, negligible quenching effect was observed when the solution of Fe^{3+} was transferred to position C (blue and green curves in Figure 2b), indicating that such luminescent quenching phenomenon was caused by the overlap of the adsorption of between compound **2** and Fe^{3+}. Notably, when the suspension of **2** was replaced by the suspension of the mixture of **2** and Fe^{3+}, the quenching behavior became more efficient (red curve in Figure 2b), revealing the existence of strong interaction between compound **2** and Fe^{3+}. Besides, the UV-*vis* absorption spectrum of Fe^{3+} had a large overlap with the excitation spectrum of **2**, indicating that the competitive absorption might be another reason for such quenching phenomenon. That is, such quenching behavior was ascribed by the synergetic effect of the competitive absorption and the energy-transfer between Fe^{3+} and the framework of **2**.

Recently, Fu' group have synthesized a novel Tb-MOF (**3**) with an ultra-high quantum yield (94.91%).[115] Compound **3** featured a 3D interpenetrating framework, where plentiful naked phenolic hydroxyls were located. Because of the presence of such exposed phenolic hydroxyls, compound **3** was considered to be a promising luminescent sensor for Fe^{3+} equipped with high sensitivity (K_{sv} = 162 570 M^{-1}) and low LOD (0.35 μM). For simple and convenient detection of Fe^{3+}, luminescent test papers were prepared and the changes in color with the addition of Fe^{3+} were easily distinguished with naked eyes. The binding energy at 532.9 eV of hydroxyl oxygen (C-OH) was found to move to 533.1 eV, indicating the presence of electronic interaction between hydroxyl supplied by phenolic hydroxyl groups and Fe^{3+}. The exci-

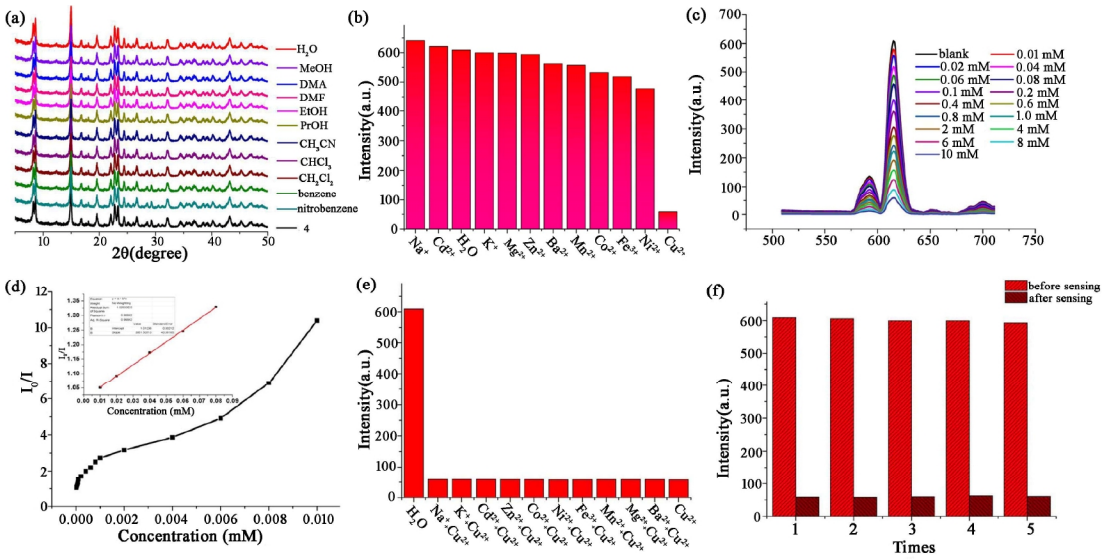

Figure 3. (a) The PXRD patterns of **4** soaked in different organic solvents. (b) Luminescent intensity at 615 nm of **4** immersed in aqueous solutions with different metal ions. (c) Luminescent spectra of **4** in aqueous solutions containing various Cu^{2+} concentrations. (d) The S-V plot of **4**. (e) Anti-interference experiment of **4**. (f) The recyclable experiments of **4** for sensing Cu^{2+}. Reproduced with permission from Ref.[116]

DOI: 10.14102/j.cnki.0254-5861.2022-0138

tation spectrum of **3** displayed an obvious overlap with the UV-*vis* absorption spectrum of Fe^{3+}, implying the existence of competitive energy absorption between **3** and Fe^{3+} ions. In conclusion, affluent active sites combined with the commonly competitive adsorption were confirmed to be responsible for such charming luminescent quenching phenomenon.

A tri-carboxylate ligand stemmed from in situ decarboxylation reaction of another tetra-carboxylate ligand was selected by Li and co-workers to fabricate a novel 3D Eu-MOF (**4**) for sensing Cu^{2+}.[116] Interestingly, compound **4** can maintain the integrity of the skeleton in water and common organic solutions (Figure 3a). Inspired by its excellent stability, the luminescent sensing experiments of metal cations were investigated. As displayed in Figure 3b, except for Cu^{2+}, other metal cations showed ignorable influence on the emission intensity of **4**. Compound **4** exhibited promising luminescent sensing ability for Cu^{2+} based on the luminescent quenching effect with the values of K_{sv} and the detection limit of 3951.5 M^{-1} and 3.3 μM through the titration experiments (Figure 3c and 3d). Also, as a potential luminescent sensor for Cu^{2+}, **4** possessed high selectivity, anti-interference ability and recyclability (Figure 3e and 3f). The presence of weak coordination interaction between Cu^{2+} atoms and the free oxygen atoms from uncoordinated carboxylate groups might impede the energy transfer from the ligand to the central Eu^{3+} ion. In addition, the partial overlap between the absorption spectrum of Cu^{2+} and

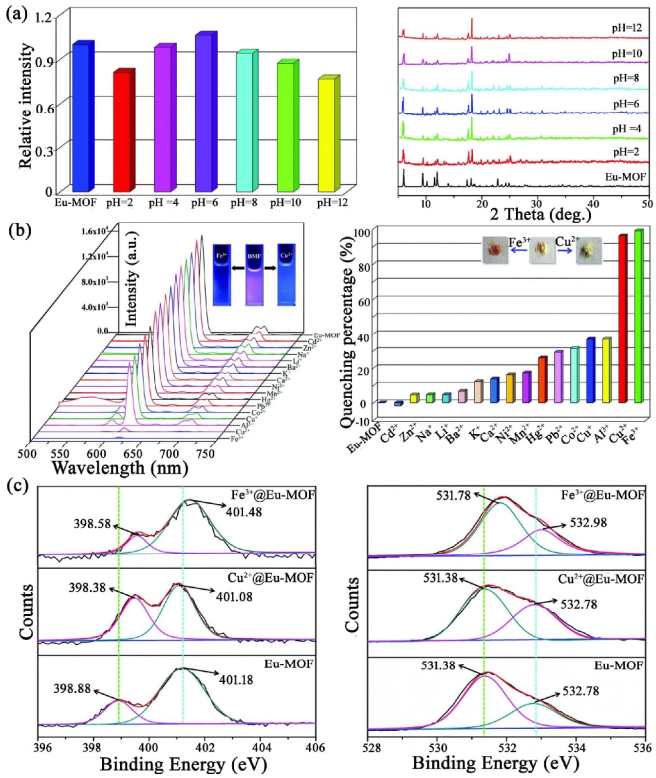

Figure 4. (a) Luminescence intensities and PXRD patterns of the **5** dispersed in aqueous solutions in the pH range of 2-12. (b) The Luminescence spectra and quenching percentage of **5** dispersed in DMF solutions with different metal cations. (c) N 1s and O 1s XPS spectra of compound **5**, Cu^{2+}@5 and Fe^{3+}@5. Reproduced with permission from Ref.[117]

the excitation spectrum of **4** might be another possible reason for the quenching effect. Therefore, the possible quenching mechanism may be the combination of the competitive adsorption and weak interaction between Cu^{2+} and the uncoordinated oxygen atoms from carboxylate groups.

A 3D supramolecular framework (Eu-MOF, **5**) connected by mixed ligands (H_4dpc and bibp) for sensitive detection Cu^{2+} and Fe^{3+} was fabricated by Yang et al.[117] In this structure, binuclear clusters ([$Eu_2(COO)_2$]) were ligated to form a 1D metal chain. The neighboring chains are further linked to a 2D layer (type A) by the dpc^{4-} ligands. Interestingly, another layer (type B) was composed by uncoordinated bibp ligands. Finally, a sandwich-shaped 3D supramolecular framework was further formed by the alternation of two kinds of layers $(\cdots A\text{-}B\text{-}A\text{-}B\cdots)_n$ through hydrogen bonding interactions. It is worth mentioning that compound **5** exhibited stable emission intensities in the pH range of 2-12 (Figure 4a). Furthermore, the emission intensity of compound **5** was obviously quenched by Cu^{2+} and Fe^{3+} without interference (Figure 4b). And the K_{sv} and LOD values of **5** were calculated to be 4.84 × 10^3 M^{-1} and 1.32 × 10^{-5} M for Fe^{3+} and 4.62 × 10^3 M^{-1} and 2.53 × 10^{-5} M for Cu^{2+}, respectively. Multiple methods, such as power XRD, UV-*vis* spectroscopy, XPS and ICP-AES, were introduced to explore the quenching mechanism (Figure 4c). When introducing Cu^{2+}, just the N 1s peaks were observed to shift from 398.88 and 401.18 eV to 399.48 and 401.08 eV, while the O 1s peaks kept unchanged, confirming the weak interaction between the N atoms and Cu^{2+}. Whereas, when Fe^{3+} was introduced, not only did the N 1s peaks shift from 398.88 and 401.18 eV to 399.58 and 401.48 eV, but also the O1s peaks shifted from 531.38 and 532.78 eV to 531.78 and 532.98 eV, respectively, indicating weak interactions of Fe^{3+} with the N and O atoms from the bibp and dpc^{4-} ligands. That is, the weak interactions between Cu^{2+}, Fe^{3+} and the Lewis active sites (N atoms) from dpc^{4-} or bibp ligands were considered as the main reason for such quenching behavior.

For efficient detection of Cd^{2+} ion, a porous Eu-MOF (**6**) built from a tetra-carboxylate ligand functionalized with amino group was synthesized by Su and co-workers.[105] In the structure of **6**, two kinds of 1D channels were found in bc layer, giving the porosity of 21% calculated by PLATON software. To explore the stability of compound **6**, the fresh samples were dispersed in water, boiling water and common organic solvents, and then the PXRD was collected. The results indicated compound **6** can retain structural integrality in such various media. Solid-state luminescent measurements of **6** displayed typical red emission of Eu^{3+} with the lifetime and quantum yield of 597 μs and 4.2%, respectively. Considering the porous stable structure and excellent luminescent properties, the exploration for metal ions was arranged. When the concentrations of metal ions were 10 mM, all five metal ions including Cd^{2+}, Al^{3+}, Cr^{3+}, Zn^{2+} and Hg^{2+} ions show non-negligible luminescent enhancing effects. Especially for Cd^{2+}, the emission intensity was increased to 23-fold compared with the original level. Whereas, the selectivity of these metal ions was barely satisfactory owing to the mutual interference among these five target ions. As the concentration of metal ions decreased to 1 mM, the mutual interference was almost eliminate

DOI: 10.14102/j.cnki.0254-5861.2022-0138

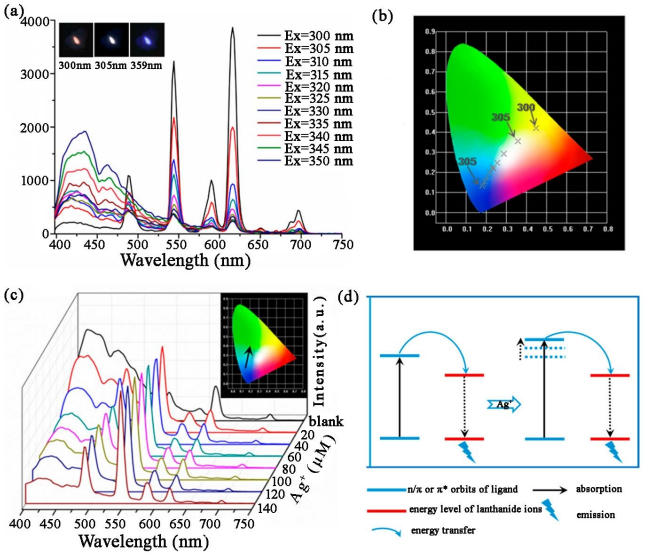

Figure 5. (a) Luminescent spectra of compound **7** as excitation wavelengths change from 300 to 350 nm. (b) The corresponding CIE chromaticity diagram. (c) Luminescent spectra of **7** with the gradual addition of Ag^+ ions. (d) Scheme for the effect of Ag^+ on the energy transfer process from ligand to central metal ions. Reproduced with permission from Ref.[118]

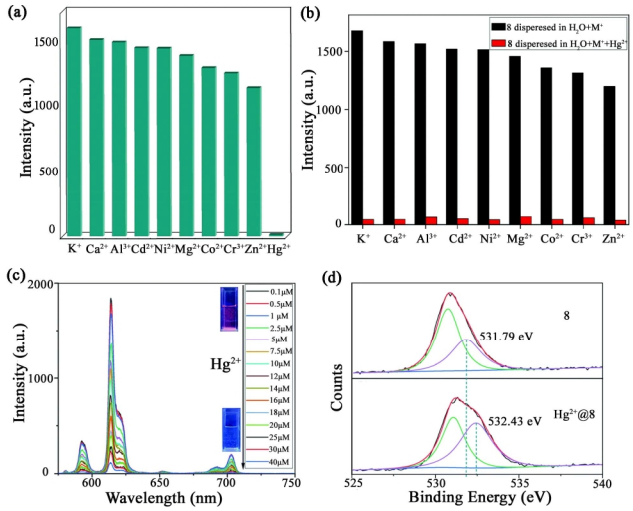

Figure 6. (a) Relative luminescent intensities of compound **8** in aqueous solutions with various metal cations. (b) Anti-interference experiments of **8**. (c) Luminescent spectra of compound **8** in aqueous solutions with various concentrations of Hg^{2+}. (d) XPS spectrum for the O 1s region of **8** before and after immersion in Hg^{2+}. Reproduced with permission from Ref.[119]

and compound **6** exerted selective luminescent detection of Cd^{2+} of Cd 3d peaks in Cd^{2+}@Eu-MOF as well as the shift of O 1s peak of Cd^{2+}@Eu-MOF from 531.5 to 531.7 Ev indicated that the interaction between Cd^{2+} and the carboxylate groups might occur, which amplified the energy transfer from the ligand to the Eu^{3+} and then enhanced the luminescent intensity of compound **6**.

In another work, a luminescence-color change (LCC) sensor for sensing Ag^+ ion was reported by Li and co-authors.[118] In the strategy of in-situ synthesis, a ternary co-doped Ln-MOF ($La_{0.88}Eu_{0.02}Tb_{0.10}$-MOF, **7**), in which the ratios of La/Eu/Tb were determined by the ICP, was obtained. Intriguingly, three isomorphic compounds displayed blue-green, red and green colors distinct by naked eyes, respectively. Moreover, as depicted in Figure 5a and 5b, when the excitation wavelengths were located at 303, 305 and 350 nm, compound **7** presented pure orange, white, and blue light, respectively. Benefited from the multi-luminescence, compound **7** might be a candidate for luminescence-color change (LCC) sensor. As expected, under the excitation at 350 nm, as the concentration of Ag^+ ion gradually increased, the blue emission tuned by the ligand was continually weaken and the typical green emission of Tb^{3+} was constantly enhanced, while no obvious variations were observed of the emission intensity of Eu^{3+} (Figure 5c). That is, as Ag^+ ions were introduced to the system, the efficiency of energy transfer process from Tb^{3+} to Eu^{3+} was hindered excited at 350 nm, resulting in the color change of compound **7** from blue to green. Additionally, as a LCC sensor for Ag^+, compound **7** was recyclable, confirmed by the consistent PXRD patterns before and after immersing in Ag^+ ions. The exploration of such LCC sensing mechanism was performed. When Ag^+ ions were introduced in the suspension of compound **7**, the emission of ligand was discovered to some degree of red shift, indicating the energy of π* ion based on the luminescent enhancing effect. The appearance orbits of the ligand was heightened and then became more matched with the resonance energy level of the Ln^{3+} ions (Figure 5d). In other words, the emission spectra of **7** in the presence of Ag^+ consist of stronger characteristic emissions of Ln^{3+} ions and weaker ligand-center emission, causing the color of **7** to turn from blue to green.

In addition, Sun et al. reported a new Eu-MOF (**8**) based on mixed organic ligands with good water stability for fast sensing and removing Hg^{2+} in water solutions.[119] Compound **8** displayed characterized red emission of center Eu^{3+} under 335 nm excitation. Featuring outstanding luminescent properties and super stabilities, the sensing experiments were executed. As described in Figure 6a, compound **8** exhibited fast and remarkable luminescent response towards Hg^{2+} based on luminescent quenching. As the concentration of Hg^{2+} increased, the luminescent intensity of **8** decreased gradually and the quenching efficiency reached up to its maximum value at the Hg^{2+} concentration of 4×10^{-2} mM, giving the Ksv and LOD values of 9.112×10^4 M^{-1} and 1.00×10^{-6} M, respectively (Figure 6c). Also, the presence of other metal ions had almost no influence on the quenching efficiency, indicating the excellent anti-interference of compound **8** on the application as luminescent probe for Hg^{2+} (Figure 6b). In addition, compound **8** had the capacity on the adsorption of Hg^{2+} with the adsorption quantity of 1.8160 mg of Hg per 100 mg. The peak of O 1s before and after immersion in Hg^{2+} solutions shifted from 531.79 to 532.43 eV, indicating the presence of strong interaction between Hg^{2+} and the O atoms from carboxylate groups of the aromatic rings, which might be responsible for such quenching behavior to Hg^{2+} (Figure 6d).

In 2020, Dai and co-workers introduced a conjugated tetracarboxylate ligand to develop a 3D Eu-MOF (**9**) constructed from

DOI: 10.14102/j.cnki.0254-5861.2022-0138

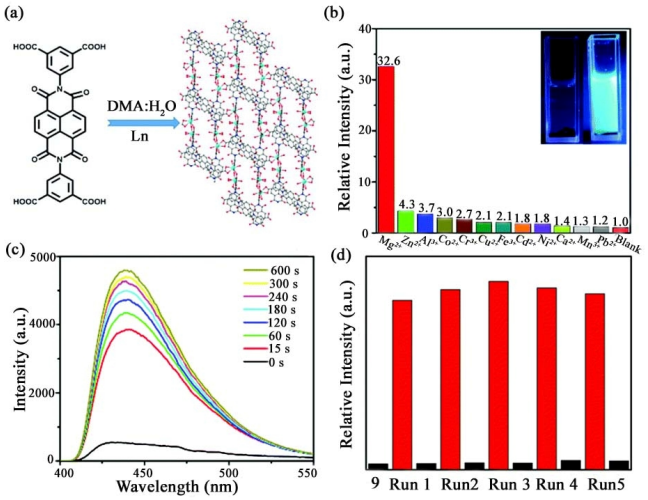

Figure 7. (a) Scheme of the synthetic strategy for compound **9**. (b) Relative luminescent intensities of **9** in solutions containing different metal cations (0.25 mmol L^{-1}). (c) Time-dependent luminescent intensities of the suspension for **9** after adding Mg^{2+} solution (200 μL). (d) The recyclable experiments of **9** for sensing Mg^{2+}. Reproduced with permission from Ref.[120]

a conjugated tetra-carboxylate ligand with a new 4,4,6-connected wxk1 topology *via* a solvent regulation strategy (Figure 7a).[120] Room-temperature luminescent spectrum in solid state of **9** showed no typical emission of Eu^{3+}, probably due to the presence of highly disordered guest solvent molecules. The suspensions of compound **9** containing diverse metal ions were prepared and the luminescent spectra were collected and compared. Different from most metal ions which show no obvious influence on the luminescence intensity of compound **9**, Mg^{2+} ions gave rise to a 10.4-fold amplification of the emission intensity with the detection limit of 1.53×10^{-10} mol/L (Figure 7b). Also, the time-dependent response of Mg^{2+} towards the emission intensity was researched, and the results indicated that when Mg^{2+} ions were added in the suspension of compound **9** just for 15 seconds, an apparent luminescent enhancing effect was observed, and the enhancing efficiency was magnified to the maximum at 600 seconds with the emission intensity by 10.4 times compared to the original value (Figure 7c). After five runs, the emission intensity and enhancing efficiency were restored (Figure 7d). The mechanism of such luminescent enhancing behavior was attributed to electron transfer interaction between the Mg^{2+} ions and the ligand, confirmed by XPS spectra of Mg^{2+}-incorporated **9**, in which a new peak at 532.1 eV assigned to O-Mg appeared, suggesting the existence of weak coordination of Mg^{2+} with O atoms in the ligand.

In addition, some other Ln-MOFs were reported and employed to detect metal cations in recent years. A Tb-MOF (**10**) with high air and hydrolytic stability was reported by Hong and co-workers.[121] Numerous Lewis basic pyridyl active sites from the ligand were uncovered inside the structure and made compound **10** a potential sensor for Fe^{3+} with high sensitivity, fast response and anti-jamming performance. Recently, a hetero-metallic luminescent probe for Fe^{3+} based on a mixed-metal organic framework (MM-MOF), Zn^{II}-Eu^{III}-MOF (**11**), was prepared by Bai' group.[122] The dynamic quenching mechanism was verified to be the main inducement by the fact that the luminescent lifetime of **11** decreased as the concentrations of Fe^{3+} increased, proving some interactions occurred between Fe^{3+} and compound **11**. And the K_{sv} and LOD values were 1.96×10^3 M^{-1} and 1.68×10^{-5} M, respectively. Another hetero-metallic anionic metal organic framework, Eu^{III}-K^{I}-MOF (**12**), as a sensitive luminescent sensor for Cu^{2+}, was reported by Yang' group.[123] Profited by its anionic framework, **12** exhibited significant adsorption capacity for Cu^{2+} (143.88 mg/g) combined with luminescence quenching. Recently, Liu and co-workers fabricated a highly water-stable Tb-MOF, (**13**), with two kinds of 1D channels, applied as luminescent sensors for Cu^{2+} based on obvious luminescent quenching effects.[124] Notably, as a selective and sensitive sensor for Cu^{2+}, compound **13** exhibited stable quenching efficiency in various media, including deionized water, tap water, and river water, with the K_{sv} and LOD in water of 4.90×10^6 M^{-1} and 1.35×10^{-9} M, respectively. In another work, two kinds of ligands (phenylmalonic acid and phenanthroline) were introduced to construct a dinuclear Tb-MOF (**14**).[125] Compound **14** possessed arresting stability in aqueous solutions in different acid and basic conditions (pH = 4, 7 or 10). Notably, luminescent sensing tests revealed that compound **14** was a promising luminescent probe for Cd^{2+} based on "turn off" effect with the LOD of 5×10^{-7} M, caused by the decomposition of Tb-MOF framework.

Sensors for Anions. Anions, essentially for biochemical processes, are commonly involved in the fields of industries and

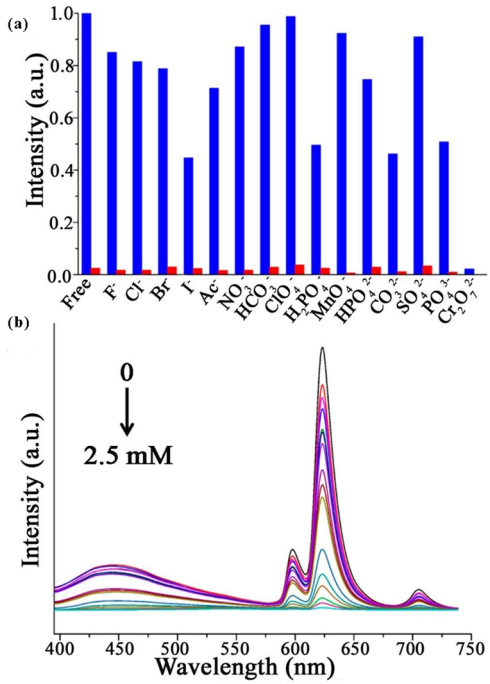

Figure 8. (a) Relative luminescent intensities of **15** soaked in various anions (1.5 mM; before (blue column) and after adding $Cr_2O_7^{2-}$ (red column)). (b) Luminescent spectra of **15** soaked in solutions with different concentrations of $Cr_2O_7^{2-}$ (λ_{ex} = 376 nm). Reproduced with permission from Ref.[135]

DOI: 10.14102/j.cnki.0254-5861.2022-0138

agricultures. Excessive anions discharged to environment can have hazardous influence on human health and ecology.[33] For instance, hexavalent chromium (Cr(VI)), designated as a human cancerogen by International Cancer Research Center and American Toxicology Organization, has serious carcinogenicity and potential teratogenicity, which mostly existed in the form of $Cr_2O_7^{2-}$ and CrO_4^{2-}. Cr(VI) can intrude into the body through the digestive tract, respiratory tract, skin and mucous membrane, leading to a series of extremely serious damage.[126-127] Thus, comprehensive attention should be paid to the development of functional sensors for effective and quantificational detecting various anions. In recent years, numerous Ln-MOFs are developed and utilized to detect anions in trace amounts.[128-134]

Gai's group reported a cationic Eu-MOF (**15**) using a viologen-based zwitterionic ligand for selective detecting $Cr_2O_7^{2-}$.[135] In compound **15**, a trinuclear cluster $[Tb_3(L)_6]$ as a secondary building unit was linked with other six neighboring trinuclear clusters through six protonated ligands. When excited at 376 nm, strong typical emission peaks of central Eu^{3+} were observed in the emission spectrum of compound **15**, revealing that europium ions can be effectively sensitized by the ligand. The detecting potential of compound **15** to anions was explored through introducing various anions to the DMF suspension of compound **15**. As shown in Figure 8a, when most anions, such as ClO_4^-, MnO_4^-, F^- and NO_3^-, were added to the suspension for compound **15**, ignorable or slight luminescent quenching effects occurred on the emission intensity of **15** by monitoring the strongest emission for Eu^{3+} at 622 nm. Notably, remarkable luminescent quenching efficiency of 97.8% was discovered as $Cr_2O_7^{2-}$ ion was injected into the prepared suspension. Further quantitative experiments were arranged to estimate the sensitivity of **15** towards $Cr_2O_7^{2-}$ ion. The results indicated that with the gradual increase of $Cr_2O_7^{2-}$ concentration from 0 to 2.5 mM, the luminescent intensity of **15** decreased gradually, giving the values for K_{sv} and LOD of 1.40×10^4 M^{-1} and the LOD of 5.6×10^{-6} M (Figure 8b). The UV-*vis* spectrum of $Cr_2O_7^{2-}$ displayed a broad overlap at 310-410 nm with the absorption of 15, implying competitive absorption between compound **15** and $Cr_2O_7^{2-}$ was considered as the primary factor for such pronounced luminescent quenching phenomenon.

Recently, another sensor for $Cr_2O_7^{2-}$ was developed by Wang's group in 2022.[136] By the reaction of $Tb(NO_3)_3{\cdot}6H_2O$ with a tricarboxylate ligand, namely 1,3,5-tris-(carboxymethoxy)benzene, a super stable Tb-MOF (**16**) was successfully synthesized. Stability experiments indicated that the structural integrity and luminescent performance of compound **16** can keep their originallevels in aqueous solution with the pH range of 3 to 12, confirming the high stability of **16** on the two aspects of structure and luminescent intensity. Encouraged by the super stability and outstanding luminescent properties, the performance of **16** on the detection for anions was explored. As shown in Figure 9a, the luminescent intensity of **16** was obviously quenched by CrO_4^{2-}/$Cr_2O_7^{2-}$ ions and the quenching efficiencies were calculated to be 99.11% and 98.81% for CrO_4^{2-} and $Cr_2O_7^{2-}$, respectively (Figure 9b). Therefore, compound **16** had the potential as a luminescent probe for CrO_4^{2-}/$Cr_2O_7^{2-}$ ions. Based on the titration tests, the quenching constants (K_{sv}) were calculated to be 1.552×10^{-4} M and 1.1134×10^{-4} M for CrO_4^{2-}/$Cr_2O_7^{2-}$ ions, respectively (Figure 9c and 9d). And the LODs were lower to be 0.65 and 0.89 μM for CrO_4^{2-}/$Cr_2O_7^{2-}$ ions, respectively (Figure 10e and 10f). Moreover, the recycling and competitive measurements manifested that compound **16** was equipped with good reproducibility and anti-interference in the application on detecting CrO_4^{2-}/$Cr_2O_7^{2-}$ ions. The quenching mechanism was also attributed to the competitive

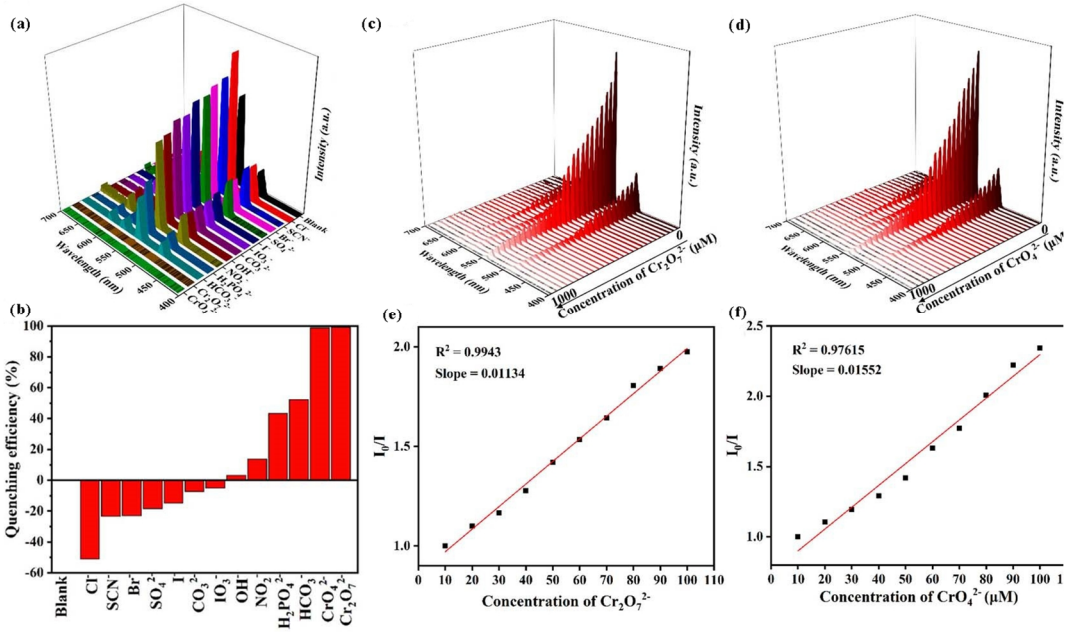

Figure 9. (a) Relative luminescent intensities of compound **16** in aqueous solutions with various anions. (b) Quenching efficiencies of compound **16** in aqueous solutions with various anions. Luminescent spectra of compound **16** in aqueous solutions with different concentrations of (c) $Cr_2O_7^{2-}$ and (d) CrO_4^{2-} ions. The S-V plots of **16** towards (e) $Cr_2O_7^{2-}$ and (f) CrO_4^{2-} ions. Reproduced with permission from Ref.[136]

DOI: 10.14102/j.cnki.0254-5861.2022-0138

absorption between compound **16** and $CrO_4^{2-}/Cr_2O_7^{2-}$ ions.

In 2019, Wang and co-workers reported a multi-responsive luminescent sensor for CrO_4^{2-}, $Cr_2O_7^{2-}$ and MnO_4^- ions based on a water-stable Eu-MOF (**17**).[137] Compound **17** exhibited a 3D porous framework with a 1D open channel, in which uncoordinated O atoms from carboxylate groups were located as open O active sites. In order to evaluate the potential of compound **17** on sensing various anions, luminescent spectra of ground samples of **17** in aqueous suspensions containing various anions (0.01 M) were monitored and analyzed. The results displayed that luminescent intensities of the suspensions with $CrO_4^{2-}/Cr_2O_7^{2-}/MnO_4^-$ ions were decreased dramatically to almost zero. Furthermore, as the concentrations of $CrO_4^{2-}/Cr_2O_7^{2-}/MnO_4^-$ anions gradually increased, the luminescent quenching efficiencies of **17** visibly enhanced, and reached their maximum values at $CrO_4^{2-}/Cr_2O_7^{2-}/MnO_4^-$ concentrations of 3.182/3.75/8.628 mM, respectively. And the K_{sv} values were $1.74 \times 10^3/1.36 \times 10^3/0.51 \times 10^3$ M^{-1} for $CrO_4^{2-}/Cr_2O_7^{2-}/MnO_4^-$, respectively. Therefore, compound **17** can act as a multi-responsive luminescent probe for $CrO_4^{2-}/Cr_2O_7^{2-}/MnO_4^-$ anions.

In another report, Liu et al. developed two isostructural lanthanide metal-organic frameworks, Eu-MOF (**18**) and Tb-MOF (**19**).[138] Single-crystal X-ray diffraction revealed compounds **18** and **19** can be simplified as a (5,7)-connected 3D framework with the point symbol of $\{3^2{\cdot}4^4{\cdot}5^4\}$ $\{3^4{\cdot}4^6{\cdot}5^6{\cdot}6^5\}$. Solid-state luminescent spectra in solid state of compounds **18** and **19** were collected. The results show that **18** exhibited typical red emission of Eu^{3+} ion peaked at 590 and 619 nm, and characteristic green emissions of Tb^{3+} ion centered at 494, 548, 588 and 624 nm were also observed in the luminescent spectrum of compound **19**. Considering the excellent luminescent properties of **18** and **19**, the luminescent sensing measurements of them towards anions were performed. Interestingly, the responses of **18** and **19** towards various anions were different. For compound **18**, the luminescent intensity was markedly quenched by $Cr_2O_7^{2-}$ ion (1 mM) with the values of K_{sv} and the detection limit of 1052 M^{-1} and 8.94×10^{-5} M, respectively; whereas, for compound **19**, a remarkable luminescent quenching effect occurred when the sample was immersed in suspension with MnO_4^- ion (1 mM), and the quenching constant (K_{sv}) and detection limit (LOD) were calculated to be 1200 M^{-1} and 4.48×10^{-5} mM. Similar luminescent quenching mechanism with other reported Ln-MOFs was confirmed: competitive adsorption between $Cr_2O_7^{2-}/MnO_4^-$ anions and compounds **18** and **19**.

Different from aforesaid luminescent sensor for MnO_4^- based on single-emission lanthanide ion, a tri-emission lanthanide metal-organic framework, $Eu_{0.06}Tb_{0.04}Gd_{0.9}$-MOF (**20**), for sensing MnO_4^- was prepared by Wang and co-workers.[139] As displayed in Figure 10a, when the excitation wavelength was adjusted from 295 to 385 nm, the color of compound **20** changed from yellow to white. That is, compound **20** was proved to be a white-light-emitting material. Besides, when dispersed in aqueous solutions with different pH, no changes were found both in the luminescent intensities and PXRD curves, demonstrating the luminescent performance and structure stability of **20**. In view of the precious white-light emission property and outstanding stability of compound **20**, the luminescent sensing tests for sensing anions were executed. The results illustrated that among all the anions, just MnO_4^- ion generated an amazing quenching effect on the luminescent intensity of **20** (Figure 10b). The high sensitivity of **20** towards MnO_4^- was verified by the luminescent titration study. With the stepwise addition of MnO_4^- concentration, the luminescent quenching phenomenon became increasingly apparent and the quenching efficiency increased rapidly, giving the K_{sv} value of

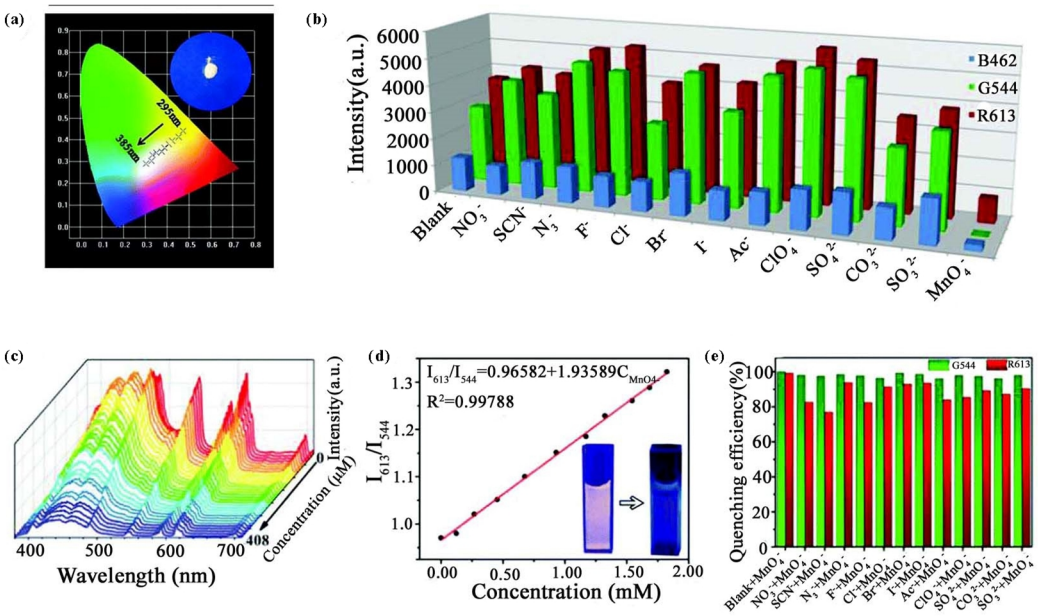

Figure 10. (a) CIE chromaticity diagram of **20** with excitation wavelengths varying from 295 to 385 nm. (b) Relative luminescent intensities of **20** immersed in the aqueous solutions containing different anions (1 mM) (λ_{ex} = 365 nm, red: 613 nm; green: 544 nm; blue: 462 nm). (c) Luminescent spectra of **20** in aqueous solution with different concentrations of MnO_4^- excited at 365 nm. (d) The S-V plots of **20**. (e) Anti-interference experiments of **20**. Reproduced with permission from Ref.[139]

DOI: 10.14102/j.cnki.0254-5861.2022-0138

1.97 × 10^{-8} M (Figure 10c). Furthermore, the anti-jamming capability and recyclability of **20** applied as a luminescent sensor for ion were also researched, and the results stated that compound **20** can be regarded as a tri-emission luminescent sensor for MnO_4^- decorated with virtues of high selectivity, good recyclability and satisfying interference immunity (Figure 10d). The overlap between the UV-*vis* absorption spectrum of MnO_4^- and the excitation/emission spectra of **20** suggested that the energy can be competitively adsorbed by MnO_4^-, leading to the luminescent quenching effect. Besides, the luminescent lifetime researches of **20** before and after being immersed in MnO_4^- indicated the presence of static quenching mechanism. Thus, dual function of competitive adsorption and the static quenching mechanism resulted in such luminescent quenching effect.

Compared with CrO_4^{2-}/$Cr_2O_7^{2-}$/MnO_4^-, the luminescent sensors for CO_3^{2-} were rarely reported. Carbonate, such as Na_2CO_3, K_2CO_3 and $(NH_4)_2CO_3$, are usually used as food additives. Excessive intake of carbonate may disrupt the hormone signaling for development and reproduction. Therefore, for detecting CO_3^{2-}, Cai et al. selected an organic ligand with a hydroxyl group, 2-(2-hydroxyphenyl)imidazo[4,5-f][1,10]phenanthroline. By the reaction of europium nitrate and the ligand, a 0D Eu-MOF (**21**) was successfully prepared.[140] In the structure of compound **21**, the hydroxyl group was failed to coordinate with the central Eu^{3+} ion. The solid-state luminescent spectrum of **21** exhibited characteristic emissions of Eu^{3+} and very weak emission of ligand

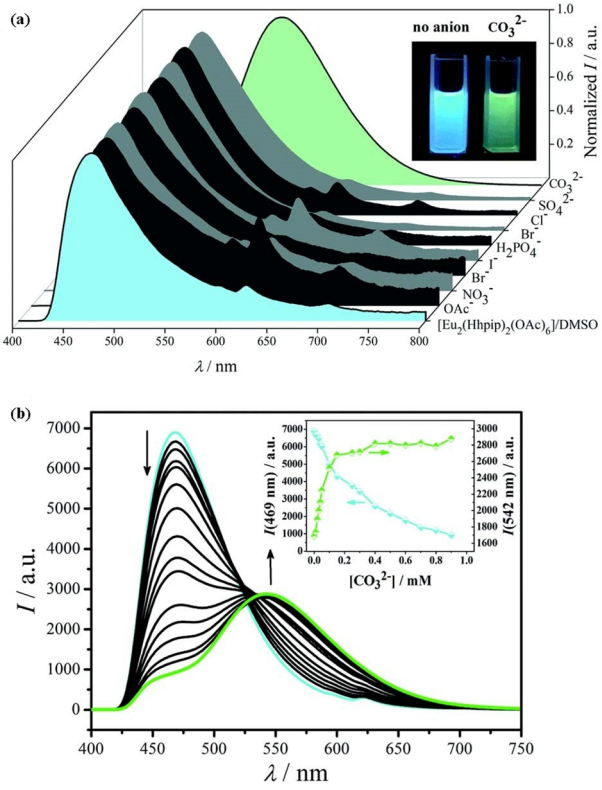

Figure 11. (a) Luminescent spectra of **21** dispersed in DMSO solution (10 μM) with various anions (1 mM) (λ_{ex} = 350 nm). (b) Luminescent spectra of **21** in DMSO solution with different concentrations of CO_3^{2-} ion (λ_{ex} = 350 nm). Reproduced with permission from Ref.[140]

was observed, implying that the selected ligand can efficiently sensitize the central Eu^{3+} ion. Interestingly, when soaked in DMSO solution (10 μM), the emissions of Eu^{3+} ion for $^5D_0 \rightarrow {}^7F_2$ transition at 624 nm and $^5D_0 \rightarrow {}^7F_5$ transition at 704 nm became very weak, and the emission of ligand centered at 470 nm became quite strong, causing the light color to turn from red to blue (Figure 11a). This phenomenon was due to the reflected solvent effect of DMSO on compound **21**, hindering the energy transfer from the ligand to Eu^{3+} ion. When introducing CO_3^{2-} ion into the DMSO solution of compound **21**, an apparent red-shift of the ligand emission centered at 470 nm appeared, and the emission color changed from blue to green distinguished by naked eyes readily (Figure 11a). Further quantitative experiments displayed that as the concentration of CO_3^{2-} ion increased, the luminescent intensity at 470 nm decreased gradually and a new emission band appeared centered at 542 nm as follows. And the LOD at 542 and 469 nm was calculated to be 12.3 or 7.8 μM, respectively. The quenching mechanism might be ascribed to the hydrogen bonding interactions: the OH groups form the phenyl groups or the imidazole NH groups can act as potential hydrogen donors to form hydrogen bonds with the CO_3^{2-} ion.

In another work, a water-stable 3D Tb-MOF (**22**) with high hydrolysis-stability for sensing nitrite ion, widely used in pickled products and ham sausages, was reported by Cheng and co-authors.[141] The typical emission peaks for Tb^{3+} centered at 489, 545, 585 and 621 nm were observed in the luminescent spectrum of compound **22** in solid-state at room temperature. The triplet state energy level T_1 of the ligand was calculated to be 22831 cm^{-1} based on the phosphorescence spectrum and the UV-*vis* spectrum of Gd-MOF at 77 K. And the energy gap △E between T_1 of the ligand and the lowest emissive level of Tb^{3+} (20500 cm^{-1}) was 2331 cm^{-1}, which fell perfectly in the range of 2500-4500 cm^{-1}, an optimal energy transfer process from the ligand to Tb^{3+} needed. The result suggested that Tb^{3+} ion can be sensitized by the ligand effectively. Luminescent sensing experiments for various salts were performed, and the results revealed different from other salts, nitrite induced an obvious luminescent quenching effect on the emission of **22** with the quenching efficiency of 83.2%, indicating it can be applied as a luminescent sensor for NO_2^- ion. Further titration tests with different volumes of NO_2^- (3, 5, and 10 μL) confirmed compound **22** can detect NO_2^- ion sensitively with the values of K_{sv} and the detection limit to be 4.82 × 10^5 M^{-1} and 28.25 nm, respectively. Additionally, anti-interference and recycling measurements verified that as a promising luminescent sensor for NO_2^-, compound **22** was recyclable at least 5 times and anti-interference. Furthermore, in order to evaluate the ability of **22** on detecting NO_2^- in practical conditions, tap water was introduced. The recoveries were calculated to be 97.7-100.9%, indicating excellent performance on sensing NO_2^- in actual conditions. The well-matched PXRD patterns before and after being immersed in NO_2^- and no obvious overlap between the UV-*vis* spectra of the ligand and $NaNO_2$ excluded the possible mechanism aroused by the collapse of the skeleton or competitive absorption. The diminishing lifetime with the increase of NO_2^- concentration revealed the presence of dynamic quenching progress. The triplet state en-

Chin. J. Struct. Chem. **2022**, 41, 2211045-2211070
DOI: 10.14102/j.cnki.0254-5861.2022-0138

ergy level T_1 of $NaNO_2$ was calculated to be 19084 cm^{-1} with the energy gap between the lowest emissive level of Tb^{3+} (20500 cm^{-1}) being 1416 cm^{-1}, indicating the existence of energy transfer between **22** and $NaNO_2$. Thus, dynamic quenching behavior occurred.

In addition, a new ligand was synthesized to construct a 3D Eu-MOF (**23**) for sensing $C_2O_4^{2-}$.[142] Luminescent sensing measurements were performed and the results indicated that compound **23** can detect $C_2O_4^{2-}$ ion with high quenching efficiency and the K_{sv} and LOD values were calculated to be 2.07×10^3 M^{-1} and 16.5 μM, respectively.

As we all know, the fast and accurate detection of ions is of great importance in human health and environmental protection. Herein, we list various luminescent sensors based on Ln-MOFs for detecting different ions, including Fe^{3+}, Cd^{2+}, Cu^{2+}, Zn^{2+}, Ag^{+}, Hg^{2+}, Mg^{2+}, $Cr_2O_7^{2-}$/CrO_4^{2-}, MnO_4^{-}, CO_3^{2-}, $C_2O_4^{2-}$ and NO_2^{-}. In the short run, the perspective of functionalized Ln-MOFs for rapid detecting various ions looks bright based on brilliant designs and strategies.

Sensors for Antibiotics

Antibiotics, a total of 20 classes containing 260 species, have been widely used in treating diseases caused by bacterial and fungal infections.[67] Whereas, only a small fraction of consumed antibiotics can be absorbed and metabolized by the body, and a large amount of the excessive antibiotics are excreted *via* urine and feces, being one of the dominating pollutants in water. The terrible thing is that varieties of antibiotics have been detected in subsidiary agricultural products, subsoil water, river water and domestic water, which can penetrate into living organisms through the food chain. Unfortunately, it is difficult to remove antibiotics and their metabolites from the environment through traditional water purification methods.[143-144] Based on the above discussion, it is very important to seek an efficient and accurate method for antibiotic detection. Recently, some luminescent sensors based on lanthanide MOFs have been explored and applied to fast and satisfactory detection for antibiotics.[145-149]

Li et al. selected a di-carboxylate ligand, 5-(4-carboxyphenyl)-picolinic acid, as an organic linker to design and construct a porous 3D Eu-MOF (**24**), containing a 1D open channel with the void ratio of 40.3%.[150] The PXRD patterns before and after dispersion in aqueous solutions with various pH (pH = 4-10) and solutions containing diverse antibiotics were found to be well matched, indicating the super stability of compound **24**. The Eu-MOF in solid state exhibited significant emission of center Eu(III) ions, peaked at 596, 619, 655 and 703 nm, assigned to the transition of $^5D_0 \rightarrow {}^7F_J$ (J = 1, 2, 3 and 4). Moreover, studies on the detection for antibiotics based on the stable and highly luminescent Eu-MOF were carried out. As shown in Figure 12a, ornidazole (ODZ) caused a remarkable luminescent quenching behavior excited at 320 nm with the K_{sv} and LOD values being 3.52×10^4 M^{-1} and 5.2×10^{-7} M, respectively. Under 359 nm excitation, the emission intensity of compound **24** was notably quenched by nitrofurantoin (NFT), giving the K_{sv} and LOD values of 2.33×10^4 M^{-1} and 4.3×10^{-7} M, respectively (Figure 12b and 12d). That is, compound **24** can be used as an effective luminescent sensor for ODZ and NFT with highly sensitive, excellent stable and anti-interference abilities. The competition adsorption between compound **24** and ODZ and NFT might be responsible for such luminescent quenching phenomenon.

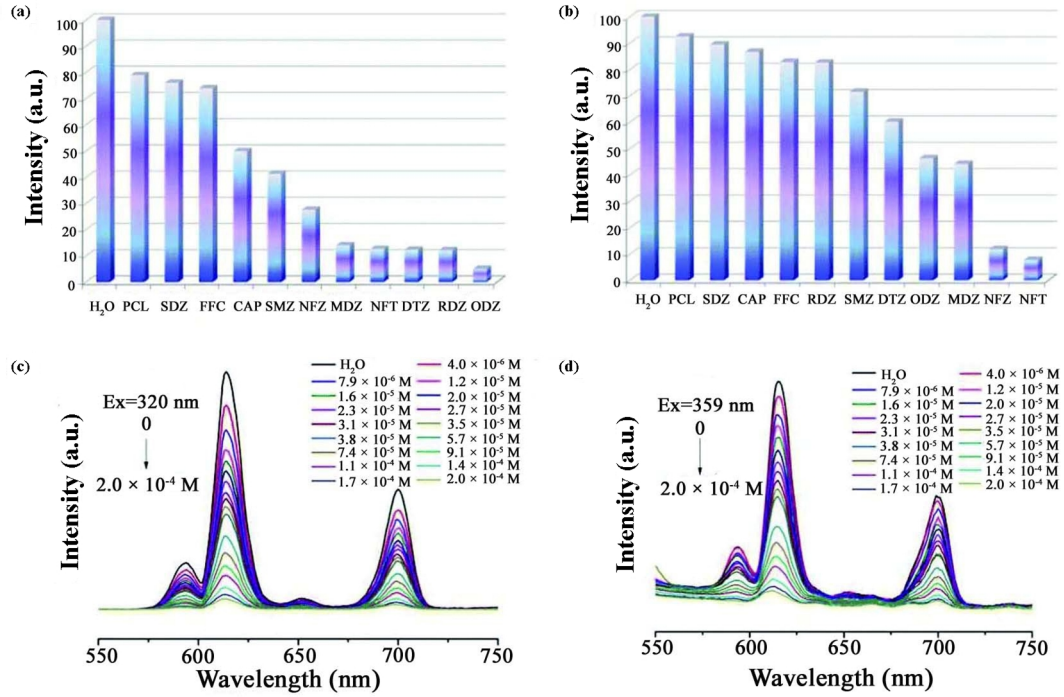

Figure 12. Relative luminescent intensities of **24** in aqueous solutions with different anions (2.0×10^{-4} M) (a) excited at 320 nm and (b) 359 nm. Luminescent spectra of **24** in solutions with various concentrations of (c) ODZ excited at 320 nm and (d) NFT excited at 359 nm. Reproduced with permission from Ref.[150]

A new tetra-carboxylate ligand functioned with urea groups, 5,5′-(((1,4-phenylenebis(azanediyl))bis(carbonyl))bis(azanediyl))-diisophthalic acid, was elaborately designed and introduced to synthesize a 3D porous framework, Tb-MOF (**25**), for detecting antibiotics by Zheng' group.[151] Beneficially, compound **25** possessed an unusually stable structure, since the PXRD patterns after being soaked with water at acid, neutral and basic conditions as well as the aqueous solutions containing various antibiotics were well-matched with that of the as-synthesized one. When excited at 336 nm, luminescent spectrum of **25** at room temperature consisted of two main kinds of emissions: one broad emission band centered at 400 nm was ascribed to the ligand and the others were attributed to the $^5D_4 \rightarrow {}^7F_J$ (J = 6-2) transitions of Tb^{3+} ion peaked at 488, 544, 585, 620, and 650 nm. Inspired by the stable structure and specific luminescent properties, the capacities of compound **25** on the detection for antibiotics were performed. Three different classes of antibiotics, including nitrofurans (NFs), nitroimidazoles (NMs) and sulfonamides (SAs), displayed distinct influence on the emission intensity of compound **25** based on the "turn on" or "turn off" effects (Figure 13a). As shown in Figure 13b, for nitrofurans (NFs), the emission for ligand at 400 nm was slightly quenched and the emissions for Tb^{3+} ions were markedly quenched. And the ratio of luminescent intensity (I_{544}/I_{400}) was discovered to stepwise increase as the concentrations of NFs were gradually added (Figure 13d). For nitroimidazoles (NMs), the variation trend of the emission intensities of ligand and Tb^{3+} ions was similar to that of nitrofurans (NFs) while the values of (I_{544}/I_{400}) decreased on the contrary with the addition of NMs; whereas, for sulfonamides (SAs), the emission intensities of ligand as well as the centered Tb^{3+} were enhanced at different degrees (Figure 13c), the I_{544}/I_{400} values of which were scarcely changed after immersion in solutions containing SAs. Further researches proved that compound **25** might be applied as a first-reported dual-emission self-calibrating luminescent sensor for differentiating such three different classes of antibiotics featuring high sensitivity, fast-response and recycle abilities (Figure 13e and 13f). To investigate the sensing mechanisms, a series of experiments were arranged. The luminescent lifetime remained unchanged before and after soaking in antibiotics, revealing that the luminescent quenching might be due to the interaction between the antibiotics and ligand instead of Tb^{3+} ion. In addition, the lower energies of LUMOs for nitro-antibiotics compared with that of the ligand gave the chance for energy transferring from the ligand to nitro-antibiotics (photo-induced electron transfer (PET)), leading to the luminescent quenching behavior. While the energy of LUMO for SOM was higher than that of the ligand, suggesting that SOM was able to be regarded as an electron donor, giving the luminescent enhancing effect. In addition, competitive absorption between nitro-antibiotics and **25** was considered as another reason for such luminescent quenching effect. Therefore, the combination of PET and the competitive absorption jointly caused the luminescence quenching effect towards the nitro-antibiotics.

Another efficient luminescent sensor for antibiotics in aqueous solution was reported by Wang and co-authors.[152] In this work, a tripodal-shaped semi-rigid ligand, 5-(4-carboxybenzyloxy)-isophthalic acid, was utilized and reacted with europium nitrate under solvothermal conditions to generate a 3D Eu-MOF (**26**) simplified to a (3,6)-connected flu-3,6-C_2/c net through the TOPOS analysis. Luminescent spectrum at room temperature of compound **26** was composed of four characteristic emission peaks of Eu^{3+} ions centered at 590, 614, 650, and 698 nm decorated with red light. No broad emission of the ligand was observed, indicating the effective "antenna effect" of the ligand to Eu^{3+} ions. Seven common antibiotics were selected to explore the potential of compound **26** on the detection for antibiotics. Most antibiotics displayed almost ignorable influence on the luminescent spectra of compound **26**. Significantly, remarkable luminescent quenching effects on the emission intensity were discovered when NFT and NZF were introduced with the quenching efficiencies of 99.65% and 99.69%, respectively. The values of K_{sv} were calculated to be 5.29 × 104 M^{-1} for NFT and

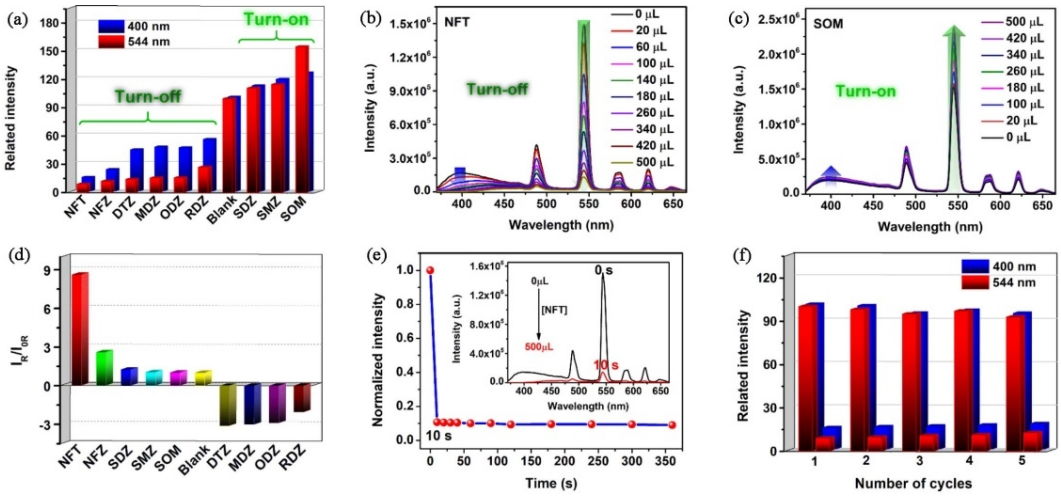

Figure 13. (a) Related luminescent intensities of **25** with different antibiotics. Luminescent spectra of **25** with different concentrations of (b) NFT and (c) SOM. (d) The I_R/I_{0R} of **25** after adding different antibiotics. (e) Luminescent response time of **25** towards NFT. (f) The recyclable experiments of **25** for NFT. Reproduced with permission from Ref.[151]

Chin. J. Struct. Chem. **2022**, 41, 2211045-2211070
DOI: 10.14102/j.cnki.0254-5861.2022-0138

4.38 × 10^4 M^{-1} for NZF. And the detection limits for NFT and NZF were 9.92 and 11.4 μM, respectively. Lower LUMO energy of NFT and NZF made the energy transfer process from the ligand to NFT/NZF, resulting in the promising sensing for NFT/NZF based on the luminescent quenching behavior.

Recently, Xu and co-workers have reported a three-dimensional Eu-MOF (**27**) constructed by a tri-carboxylate ligand, 4,4′,4″-s-triazine-2,4,6-tribenzoic acid.[153] Interestingly, compound **27** possessed excellent structural stability and luminescent stability in acid and basic aqueous solutions with pH range of 2-14 as well as in diverse common organic solvents. Therefore, the luminescent sensing abilities of compound **27** towards antibiotics were estimated and the results revealed that tetracycline hydrochloride (TCH) had a dramatically quenching effect on the emission intensity of compound **27**. The values of K_{sv} and LOD (the detection limit) were calculated to be 3.09 × 10^5 M^{-1} and 7.35 ppm, respectively. Additionally, the luminescent intensity and quenching efficiency can restore their original levels after five cycles, indicating compound **27** might be applied as a promising luminescent probe for TCH with satisfactory regeneration and stability. The lower LUMO energy as well as the overlap between the UV-*vis* absorption spectra of TCH and the excitation spectrum of compound **27** led to the luminescent quenching effect. That is, the combined action of photo-induced electron transfer (PET) and competitive absorption between **27** and TCH was regarded as the main inducement for such quenching phenomenon.

In addition, some other Ln-MOFs were reported and engaged in the application as luminescent sensors for detecting antibiotics in recent years. In 2019, Gao et al. reported a water-stable 2D Dy-MOF (**28**) decorated with two different emission bands at 385 nm for the ligand and 481 and 573 nm from the centered Dy(III).[154] Therefore, compound **28** was utilized as an effective ratio-metric luminescent probe for FZD and NFZ with the detection limit of 0.0476 μM for FZD and 0.0482 μM for NFZ (Figure 14). At the same time, Li's group synthesized an anionic Tb-MOF by the reaction of terbium nitrate and a tri-carboxylate ligand, 3-(3,5-dicarboxylphenyl)-5-(4-carboxylphenl)-1H-1,2,4-triazole). And a host-guest composite, RhB@Tb-MOF (**29**), was obtained by incorporating a cationic dye of rhodamine B (RhB) *via* cation exchange process.[155] The solid-state emission spectrum of compound **29** was composed of relatively weak emission of Tb^{3+} ions peaked at 545 nm and quite strong emission at 630 nm derived from RhB. Notably, nitrofuran antibiotics (NZF and NFT) represented remarkable luminescent quenching behavior on the luminescent intensity of **29** by monitoring the $^5D_4 \rightarrow {}^7F_J$ transition of Tb^{3+} ion at 545 nm, and the quenching efficiency was gradually enhanced as the concentrations of NZF and NFT slowly increased, giving the detection limit of 0.502 and 0.448 μM for NZF and NFT monitored at 545 nm, respectively. Additionally, when quinolone antibiotics such as CPFX and NFX were added to the system of **29**, distinguishing changes of the luminescent colors were observed by naked eyes from yellow to white to blue with the addition of CPFX and NFX concentrations. In 2020, Liu and co-authors employed an organic ligand, 2-(4-pyridyl)-terephthalic acid, to design and form a 3D Tb-MOF (**30**) with excellent stability in acid and basic water and common organic solvents.[156] Thanks to the abnormal stability and promising luminescent performance, compound **30** exhibited adequate luminescent quenching effects for nitrofuran (NIF) with the detection limit and K_{sv} of 1.1 × 10^4 M^{-1} and 8.1 × 10^{-5} M, respectively. In

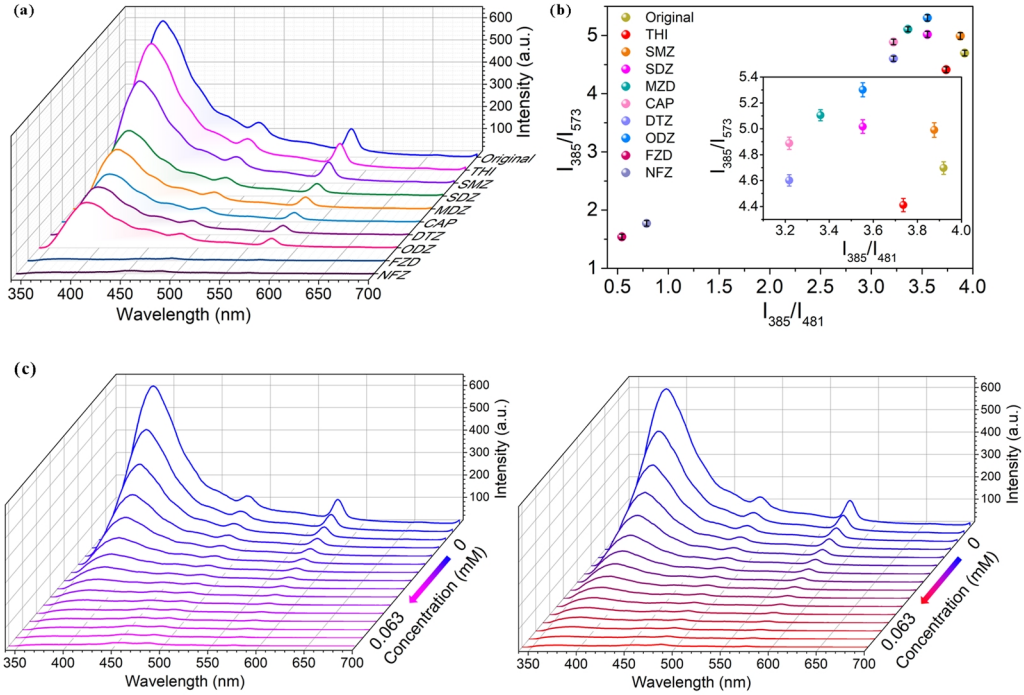

Figure 14. (a) Luminescent spectra of **28** for different antibiotics (1 mM) in water solutions (λ_{ex} = 315 nm). (b) Decoded map for different antibiotics (0.1 mm) based on the ratios of I_{385}/I_{481} and I_{385}/I_{573}. Luminescent spectra of **28** soaked in water with different concentrations of (c) NFZ and (d) FZD. Reproduced with permission from Ref.[154]

DOI: 10.14102/j.cnki.0254-5861.2022-0138

another research, Wang and co-workers reported a 2D Eu-MOF (**31**) taken on two different forms, needle-shaped colorless crystals (20-80 μm) and colorless power (2 μm).[157] The Eu-MOF power displayed super structure stability and luminescence stability in water. Luminescent detection on sensing antibiotics disclosed compound **31** had the capacity on effectually sensing for sulfamethzine (SMZ) with high sensitivity and anti-interference, giving the values of K_{sv} and detection limit to be 4.598 × 10^4 M^{-1} and 0.6554 μM, respectively. Cooperative effect of the electron transfer and inner-filter effect (IFE) was considered as the predominant impetus for the luminescent sensing effect towards SMZ.

Herein, we summarize various Ln-MOFs for sensing antibiotics, including ODZ, NFT, SOM, NZF, TCH, FZD, NFZ, NIF and SMZ. Luminescent sensors for antibiotics based on Ln-MOFs exhibit lots of advantages, such as fast-response, high sensitivity, real-time detection, and so on. It is worthy of trust that Ln-MOFs applied as potential luminescent sensors for antibiotics will have a promising future.

Sensors for Amino Acids

As we know, there are more than 20 kinds of amino acids in human body, including eight essential amino acids, which are unable to synthesize by self and have to uptake from daily diet. Importantly, amino acids are primary substances for the establishment of proteins, cells and tissues.[73,158] The balance of various amino acids is a prerequisite for human health since amino acids are involved in almost all physiological activities in body. Notably, any deficiency of amino acid can impact the normal functions of immune system.[74-75] In recent years, the contents of amino acids or their metabolites in serum have become an important indicator for disease screening.

A new microporous terbium-based metal-organic framework, Tb-MOF (**32**), was designed and prepared for detecting glutamic acid (Glu) by Zhang and co-authors.[159] In the structure of compound **32**, two kinds of cages, tetrahedral and octahedral, were constructed: the tetrahedral one was linked by four hexa-nuclear $[Tb_6(\mu_3\text{-}OH)_8(CO_2)_{12}]$ clusters (hexa-nuclear SBUs) and six ligands with the size of 5.3 Å, and the octahedral one was formed through six hexa-nuclear SBUs and twelve ligands with the size of 7.5 Å. The porous properties of **32** were confirmed by the N_2 adsorption tests, giving the BET surface area and pore volume of 613.6 $m^2 \cdot g^{-1}$ and 0.244 $cm^3 \cdot g^{-1}$, respectively. The room-temperature luminescent spectrum of the suspension of compound **32** displayed dual emissions originated from the ligand centered at 430 nm and central Tb^{3+} ions peaked at 488, 544, 583 and 621 nm. Benefited from the high linkage of hexa-nuclear SBUs and ligands, compound **32** possessed extraordinary chemical stability and light resistance. By virtue of the super stability and dual emissions, the potential of compound **32** as a self-calibrated sensor for Glu was explored. As the solutions of Glu were dropwise added to the suspension of **32**, no significant changes were found in the emission intensity of Tb^{3+} ions, while the emission of the ligand at 430 nm was obviously enhanced (Figure 15a). Thus, compound **32** might be utilized as self-calibrated luminescent sensor relying on the self-regulation through the combination of the detected signal (ligand-related emission) and the reference (Tb^{3+} centered emission). The ratio of emission intensity at 430 and 544 nm (I_{430}/I_{544}) was equated to a well-fitted linear relationship with the concentrations of Glu, giving the value of the detection limit of 3.6 μM (Figure 15b). Moreover, the color of compound **32** was observed to gradually change from green to greenish-blue to blue by naked eyes, indicating the capacity of compound **32** on colorimetric luminescent sensing for Glu. Additionally, the toxicology and selectivity measurement of compound **32** indicated that as a potential luminescent sensor, compound **32** is highly selective in biological environment with anti-jamming capability (Figure 15c and 15d). Finally, a simple and convenient one-to-two decoder logic gate was fabricated based on the concentration of Glu as the input signal and the ratio of I_{430}/I_{544} as output signals (Figure 16). Because the dangerous threshold limit value for Glu was 19.2 × 10^{-5} M, the emission at this concentration was selected as a danger threshold. When the input concentration of Glu was below 19.2 × 10^{-5} M, the normal gate

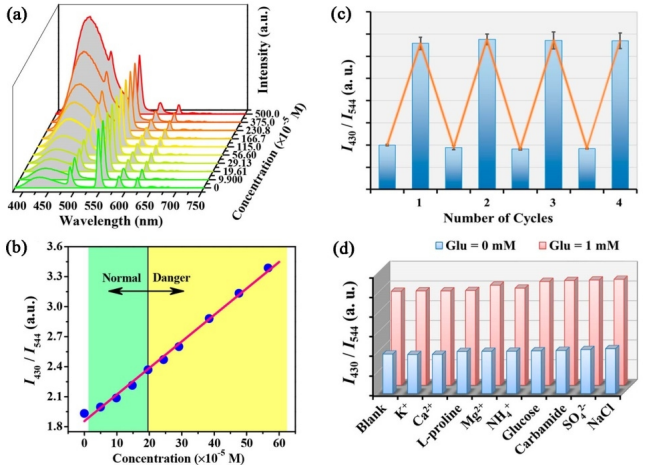

Figure 15. (a) Luminescent spectra of **32** with different concentrations of Glu (0-5 mM). (b) The linear relationship between I_{430}/I_{544} of **32** and Glu concentrations. (c) The recyclable experiments of **32** for Glu. (d) Anti-interference experiment of **32** to Glu. Reproduced with permission from Ref.[159]

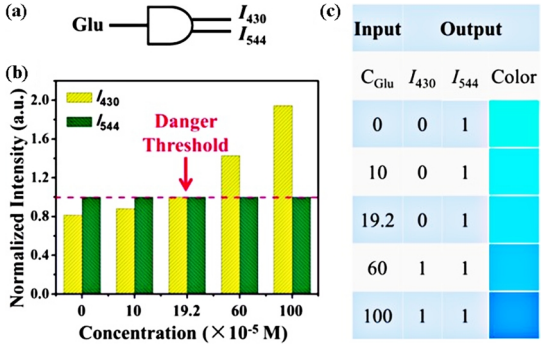

Figure 16. (a) One-to-two decoder logic gate (Input signals: Glu concentrations; Output signals: the luminescent intensities of **32** at 430 nm and 544 nm. (b) Relative luminescent intensities of **32** as the concentrations of Glu at none, normal, dangerous threshold limit value, and danger. (c) Truth table and output color of the logic analytical device for Glu monitoring. Reproduced with permission from Ref.[159]

DOI: 10.14102/j.cnki.0254-5861.2022-0138

was triggered. While the input concentration overstepped the critical value, the Danger gate was activated, suggesting the simple and real-time detection for Glu.

Zhu et al. developed a 3D Tb-MOF (**33**) with a $(4^{13}\cdot6^2)(4^8\cdot6^6\cdot8)$ topological net.[160] When excited at 335 nm, **33** presented a typical green emission of Tb^{3+} with the emission peaks centered at 489, 543, 587 and 620 nm coming from the characteristic transitions of $^5D_4 \rightarrow {}^7F_J$ (J = 6 to 3) for central terbium ions. In view of the outstanding luminescent properties of compound **33**, the potential application of **33** on sensing amino acids was explored. Different aqueous suspensions of **33** containing 11 kinds of amino acids at 1.0×10^{-3} M were prepared and the luminescent intensities at 543 nm of them were monitored and analyzed. Different from other suspensions, the suspension containing aspartic acid exhibited an arresting quenching effect on the luminescent intensity of **33**. Additionally, with the gradual addition of aspartic acid, the luminescent intensities decreased gradually. And the values of K_{sv} and the detection limit were calculated to be 9.80×10^3 M^{-1} and 7.95×10^{-6} M, respectively. Thus, compound **33** can be applied as a promising luminescent sensor for aspartic acid with high selectivity and freedom from jamming. The linear relationship between the emission intensity and the concentration of aspartic acid as well as the decrease of the luminescent lifetime with aspartic acid indicated that such luminescent quenching behavior may be resulted from the presence of the interaction between aspartic acid and the framework of **33**.

Another sensor for aspartic acid based on a Tb-MOF (**34**) constructed from a tetra-carboxylate ligand functionalized with a pyrene ring was covered by Wen' group.[161] Compound **34** featured a water-stable 3D microporous structure with the void ratio of 20.40% through PLATON software. Only a broad emission band centered at 490 nm was observed in the solid state, owing to the strong coordination between Tb^{3+} ions and the conjugated ligand, thus increasing the electron delocalization. The higher lifetime of Tb-MOF than that of the ligand verified the presence of energy transfer between Tb^{3+} and the ligand. Eleven kinds of amino acids were selected to investigate the potential of compound **34** as a luminescent sensor for amino acids. It was seen that the emission intensity was significantly enhanced by aspartic acid (Asp), and the luminescent enhancing effects can be observed by naked eyes under 365 nm UV irradiation. Quantitative and competitive experiments indicated that Asp can be selectively detected by compound **34** without disturbance by most amino acids, with a relative lower LOD of 0.025 ppm. Additionally, the singlet-state (S_1) of Asp (46512 cm^{-1}) was calculated to be higher than that of the ligand (25641 cm^{-1}) through the UV adsorption spectra, indicating the energy transfer could occur from Asp to the ligand, which might be the major mechanism for such luminescent enhancing effect for Asp.

Except for Eu- and Tb-functionalized MOFs, at another work, Jiang and co-workers reported a 3D Sm-centered lanthanide MOF, Sm-MOF (**35**), by the reaction of samarium nitrate and a tetra-carboxylate ligand, 1,2,4,5-benzenetetracarboxylic acid.[162] PXRD patterns were collected to confirm the stability of samples immersed in acid and basic water solutions. The results indicated compound **35** can maintain the integrity of the framework in water with pH range of 3-11. The emission spectrum of compound **35** was collected with three strong peaks centered at 562, 598 and 646 nm corresponding to the typical transitions of $^4D_{5/2} \rightarrow {}^6H_J$ (J = 5/2, 7/2 and 9/2) for Sm(III) ions, revealing the effective "antenna effect" of the ligand to transfer the absorbed energy to central Sm(III) ions. The luminescent sensing potential of **35** on amino acids was investigated: several analysts including common ions, proteins and amino acids were selected to prepare suspensions through ultrasonic treatment, and then the luminescent response of compound **35** towards various analysts was recorded. The results displayed in Figure 17a indicated that most analysts show almost ignorable influence on the luminescent

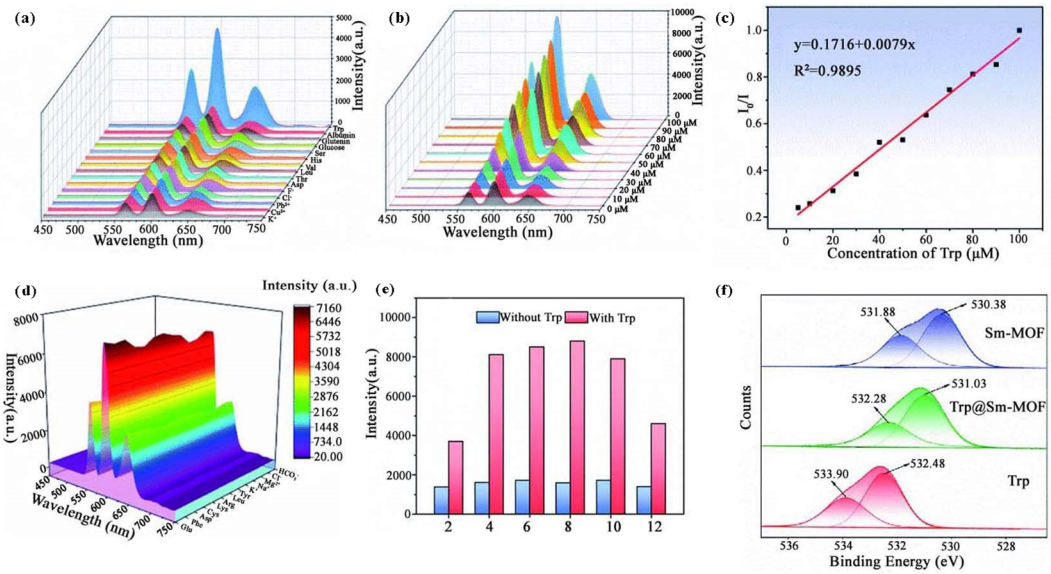

Figure 17. (a) Luminescent spectra of **35** in different amino acids. (b) Luminescent spectra of **35** after introducing Trp with different concentrations. (c) The S-V plot of **35**. (d) Anti-interference experiment of **35**. (e) Luminescent intensities of **35** for sensing Trp at different pH values. (f) The XPS spectra in the O 1s region of **35**, Trp@**35** and Trp. Reproduced with permission from Ref.[162]

DOI: 10.14102/j.cnki.0254-5861.2022-0138

intensity of **35**, while a remarkable enhancement occurred in the presence of L-tryptophan (Trp), implying the promising potential of **35** on the detection for Trp. The selectivity tests of **35** towards Trp were arranged, and the luminescent intensity exhibited a well-fitted linear relationship with the concentration of Trp at 0-100 mM with the detection limit of 330 nM (Figure 17c and 17d). Moreover, the luminescent enhancing effects were also observed when the pH of the reaction system fell in the range of 2-12, revealing that compound **35** can detect Trp in wide acid and basic conditions (Figure 17e). Furthermore, the enhancing effect was obviously observed when the Trp was introduced just for 1 minute and the enhancing efficiency reached up to the maximum after immersing for 5 minutes. As discussed above, compound **35** can be considered as a sensitive, stable and fast-responsive luminescent sensor for Trp. Additionally, milk was introduced to estimate the performance of **35** on sensing Trp in actual conditions. The recoveries were calculated to be between 93.8% and 102.9% with the relative standard deviations (RSD) lower than 4.3%, confirming compound **35** can detect Trp in actual conditions. The well matched relationship between the triplet energy (T_1) of Trp (21 260 cm^{-1}) and the emissive level of Sm^{3+} (17 900 cm^{-1}) indicated that Trp molecule could be able to act as the second "antenna molecule" to effectively transfer more energies to Sm^{3+}, resulting in such luminescent enhancing effect on Trp. In addition, the rigid indole group in the structure of Trp could efficiently decrease the occurrence of energy loss processes, such as molecular vibration and intermolecular interaction, and then cause the high-efficient energy transfer from Trp to Sm^{3+}.

In addition, a 2D La-MOF (**36**) built from an organic linker containing tetrazole and carbolxylate units was prepared under solvothermal conditions for detecting L-Tyr.[163] As-synthesized samples of **36** were dispersed in diverse solvents and the PXRD curves were collected to assess the stability of compound **36**. PXRD patterns after soaking in these solvents were well-fitted with the original pattern of the as-synthesized samples, displaying the high stability of **36**. Luminescent sensing researches were arranged and the result displayed that the luminescent intensity of compound **36** was completely quenched when L-Tyr was introduced. And the quenching constant (K_{sv}) and limit of detection (LOD) were found to be 1.40×10^4 M^{-1} and 3.60×10^{-6} M, respectively. Additionally, compound **36** was also discovered to be able to sense antibiotic nitrofurantoin (NFT) sensitively with the quenching constant (K_{sv}) and limit of detection (LOD) found to be 3.00×10^3 M^{-1} and 1.70×10^{-5} M, respectively. The luminescent lifetime decreased as the concentration of L-Tyr was increased, indicating the possible presence of hydrogen bonding interaction, that is, such luminescent quenching effect was ascribed to the dynamic quenching mechanism.

In conclusion, several Ln-MOFs were used as luminescent probes on the detection of amino acids, including Asp, Glu, Trp and Tyr. Compared with ions and antibiotics, Ln-MOFs as luminescent sensors for amino acids have not been widely developed and reported until now. Therefore, most attentions should be focused on the preparation and exploration of functionalized Ln-MOFs with fast and precise detection for amino acids.

Sensors for Other Analytes

Apart from the application on the detection of inorganic ions, antibiotics and amino acids, luminescent Ln-MOFs have been widely developed and utilized as potential chemical sensors for pesticide,[164-166] temperature[60-63] and humidity[167-168].

For efficiently detecting pesticide 2,6-dichloro-4-nitroaniline (DCN), Jiao and co-authors introduced a rigid penta-carboxylate ligand 3,5-di(2′,4′-dicarboxylphenyl)benzoic acid to design and synthesize a 3D Tb-MOF (**37**).[164] Compound **37** displayed good water stability and pH stability. When excited at 311 nm, compound **37** exhibited strong characteristic green-emission of Tb^{3+} peaked at 495, 551, 590, and 627 nm. Based on further exploration on the capacity of **37** on luminescent sensing pesticides, a series of tests were arranged and the results indicated that compound **37** presented great potential on sensing pesticide DCN in aqueous solution, giving the quenching constant (K_{sv}) and the detection limit (LOD) of 6.42×10^4 M^{-1} and 1.4×10^{-7} M. In addition, Yan' group reported a Tb^{3+}-functionalized Cd-MOF, Tb^{3+}@Cd-MOF (**38**), for detecting the biomarkers of Fungicides (3,5-dichloroaniline, 3,5-DCA) and herbicides (3,4-dichloroaniline, 3,4-DCA).[166] It is worth to mention that **38** was obtained *via* cation-exchange process: the $[(CH_3)_2NH_2]^+$ cations occupied in the open channel of Cd-MOF were replaced by Tb^{3+} ions through immersing Cd-MOF in the DMF solution of Tb^{3+} (10^{-2} M). Compound **38** was proven to be able to sensitively detect 3,4-DCA and 3,5-DCA in DMF with the K_{sv} and LOD of 25.11 and 0.0033 $mg \cdot mL^{-1}$ for 3,4-DCA and 30.21 and 0.0026 $mg \cdot mL^{-1}$ for 3,5-DCA, respectively. Furthermore, when urine samples were introduced, the values of K_{sv} and LOD for 3,4-DCA and 3,5-DCA were similar to those in DMF, indicating **38** can be applied as a candidate for sensing 3,4-DCA and 3,5-DCA in practical conditions.

A Eu^{3+}/Tb^{3+}-mixed MOF, $Eu_{0.036}Tb_{0.964}$-MOF (**39**), based on the thermally and chemically stable Eu-MOF and Tb-MOF, was reported by Su and co-workers.[60] Compound **39** was proved to act as a ratiometric luminescent thermometer at a wide temperature range from 77 to 377 K. Notably, the temperature and the ratio (I_{545}/I_{614}) of the luminescent intensity at 545 nm for Tb^{3+} and 614 nm for Eu^{3+} exhibited a good linear relationship at the range of 220-310 K, and the maximum relative sensitivity (S_m) was calculated to be 9.42% K^{-1} at 310 K. Moreover, as the temperature increased from 77 to 377 K, the luminescent colors of **39** can be distinguished by naked eyes from green to yellow and to red at last with increasing temperature, indicating the potential of the mixed compound on the application as a sensitive ratiometric temperature sensor. Besides, different from the Eu^{3+}/Tb^{3+}-mixed luminescent thermometer, Murugesu' groups prepared a 5%Yb^{3+}-doped Nd-MOF, Yb^{3+}/Nd^{3+}-MOF (**40**), as a near-infrared luminescence thermometry.[61] Interestingly, when excited at 365 nm, as the temperature increased from 15 to 300 K, the luminescent intensity of the $^4F_{3/2} \rightarrow {}^4I_{11/2}$ transition for Nd^{3+} was observed to manifold: the luminescent intensity at 1066 nm decreased, while the luminescent intensity at 1082 nm increased in the temperature range of 15 to 300 K. A well-fitted linear correlation was observed between the temperature and the luminescent intensity ratio (I_{1082}/I_{1066}). However, under 808 nm excitation, as the temperature increased from 15 to 300 K, the luminescent intensity of the $^4F_{5/2} \rightarrow {}^4I_{7/2}$ transition at 980 nm for Yb^{3+} and the

DOI: 10.14102/j.cnki.0254-5861.2022-0138

Table 1. Summaries of Mentioned Ln-MOFs, Relative Ligands and Sensing Targets

Sensing target	Ln-MOFs	Ligands	Refs.
Fe^{3+}	$H_3O[Tb(H_2O)_2(L)]$ **1**	H_4L = 4′,4‴,4⁗,4⁗′-(ethene-1,1,2,2-tetrayl)tetrakis([1,10-biphenyl]-4-carboxylic acid))	112
	$\{[Eu(L)(H_2O)]\cdot 4H_2O\}_n$ **2**	H_3L = 5-(2′,5′-dicarboxylphenyl)picolinic acid	113
	$Tb_2(L)_3(DMF)_4$ **3**	H_2L = 2-hydroxyterephthalic acid	114
	$\{[Me_2NH_2][TbL]\cdot 2H_2O\}_n$ **10**	H_4L = 1-(3,5-dicarboxylatobenzyl)-3,5-pyrazole dicarboxylic acid	121
	$[Zn_3Eu_2(L)_2(H_2O)_6]\cdot 6H_2O$ **11**	H_6L = 1,3,5-triazine-2,4,6-triamine hexaacetic acid	122
Cu^{2+}	$\{[Eu_2(L)_2(H_2O)_5]\cdot 3H_2O\}_n$ **4**	H_3L = 5-(3′,5′-dicarboxylphenyl)picolinic acid	115
	$\{[Eu(L)(2H_2O)]\cdot(Hbibp)_{0.5}\}_n$ **5**	H_4L = 2-(3′,4′-dicarboxylphenoxy) isophthalic acid; bibp = 4,4′-bis(imidazolyl)biphenyl	116
	$\{[Eu_2K(L)_4(C_2H_5OH)]\cdot(H_3O)\cdot(H_2O)_x\}_n$ **12**	H_2L = 2,2′-bipyridine-6,6′-dicarboxylic acid	123
	$\{[Eu(HL)]\cdot 3DMF\cdot 3H_2O\}_n$ **13**	H_4L = 1,4-bis(2′,2″,6′,6″-tetracarboxy-1,4′:4,4″-pyridyl)benzene	124
Cd^{2+}	$\{(Me_2H_2N)[Eu(L)]\cdot DMF\cdot H_2O\}_n$ **6**	H_4L = 2′-amino-[1,1′:4′,1″-terphenyl]-3,3″,5,5″-tetracarboxylic acid	117
	$[Tb_2(L)_4(phen)_2(NO_3)_2]$ **14**	HL = phenylacetic acid, phen = 1,10-phenanthroline	125
Ag^{+}	$[La_{0.88}Eu_{0.02}Tb_{0.10}(L)(DMF)_2]_n\cdot H_2O\cdot 0.5DMF$ **7**	H_3L = 4-(3,5-dicarboxylatobenzyloxy)-benzoic acid	118
Hg^{2+}	$\{[Eu_4(L)_6(phen)_4]\cdot m(H_2O)(phen)\}_n$ **8**	H_2L = thiobis(4-methylene-benzoic acid); phen = 1,10-phenanthroline	119
Mg^{2+}	$\{[Eu_2(L)_{1.5}(DMA)_3(H_2O)_2]\cdot 2DMA\cdot 2H_2O\}_n$ **9**	H_4L = benzo-imide-phenanthroline tetracarboxylic acid	120
$Cr_2O_7^{2-}$	$\{[Eu_3(L)_3(NO_3)_7]\cdot NO_3\cdot ClO_4\}_n$ **15**	H_2LCl_2 = 1,1′-bis(4-carboxyphenyl) (4,4′-bipyridinium) dichloride	135
$CrO_4^{2-}/Cr_2O_7^{2-}$	$\{[Tb(L)(H_2O)_2]\cdot 2H_2O\}_n$ **16**	H_3L = 1,3,5-tris-(carboxymethoxy)benzene	136
$CrO_4^{2-}/Cr_2O_7^{2-}/MnO_4^{-}$	$\{[Eu(L)(H_2O)_2]\cdot 5H_2O\}_n$ **17**	$H_4L^+Cl^-$ = 1,3-bis(3,5-dicarboxyphenyl)imidazolium chloride	137
$Cr_2O_7^{2-}$	$\{[Eu_2(L)_2(H_2O)_2]\cdot 5H_2O\cdot 6DMAC\}_n$ **18**	H_3L = 4,4′-(((5-carboxy-1,3-phenylene)-bis(azanediyl))bis(carbonyl)) dibenzoic acid	138
MnO_4^{-}	$\{[Tb_2(L)_2(H_2O)_2]\cdot 5H_2O\cdot 6DMAC\}_n$ **19**	H_3L = 4,4′-(((5-carboxy-1,3-phenylene)bis-(azanediyl))bis(carbonyl)) dibenzoic acid	138
MnO_4^{-}	$[Eu_{0.06}Tb_{0.04}Gd_{0.9}(HL)_{1.5}(H_2O)(DMF)]\cdot 2H_2O$ **20**	H_3L = 5-(3′,5′-dicarboxylphenyl) nicotinic acid)	139
CO_3^{2-}	$[Eu_2(Hhpip)_2(OAc)_6]$ **21**	Hhpip = 2-(2-hydroxyphenyl)imidazo[4,5-f]-[1,10]phenanthroline)	140
NO_2^{-}	$\{[Tb(L)(OA)_{0.5}(H_2O)_2]\cdot H_2O\}_n$ **22**	H_2L = chelidonic acid, H_2OA = oxalic acid	141
$C_2O_4^{2}$	$[Ln(L)(DMF)(H_2O)(COO)]_n$ **23**	H_2L = 4,4-(9,9-dimethyl-9H-fluorene-2,7-diyl) dibenzoic acid	142
ODZ/NFT	$[Eu(L)(OH)]\cdot xS$ **24**	H_2L = 5-(4-carboxyphenyl)picolinic acid, S = solvent molecule	150
NFT/SOM/DTZ	$\{[Tb\text{-}(HL)(H_2O)_2]\cdot x(solv)\}_n$ **25**	H_4L = 5,5′-(((1,4-phenylenebis-(azanediyl)) bis(carbonyl))bis(azanediyl))diisophthalic acid	151
NFT/NZF	$\{[Eu_2L_2(DMF)_4]\cdot xDMF\cdot yH_2O\}_n$ **26**	H_3L = 5-(4-carboxybenzyloxy)isophthalic acid	152
TCH	$\{[Eu(L)(H_2O)]\}_n$ **27**	H_3L = 4,4′,4″-s-triazine-2,4,6-tribenzoic acid	153

DOI: 10.14102/j.cnki.0254-5861.2022-0138

NFZ/FZD	$[Dy(L)(DMF)_3]_n$ **28**	H_3L = 1,3,5-tris(1-(2-carboxyphenyl)-1H-pyrazol-3-yl)	154
NZF/NFT	$RhB@[Me_2NH_2][Tb_3(L)_3(HCOO)]\cdot DMF\cdot 15H_2O$ **29**	H_3L = 3-(3,5-dicarboxylphenyl)-5-(4-carboxylphenl)-1H-1,2,4-triazole	155
NIF	$[Tb(HL)(C_2O_4)]\cdot 3H_2O$ **30**	H_2L = 2-(4-pyridyl)-terephthalic acid, C_2O_4 = oxalic acid	156
SMZ	$\{Eu(L)DMF\}_n$ **31**	H_3L = 1,3,5-tris(4-carboxyphenyl)benzene	157
Glu	$[(CH_3)_2NH_2]_2[Tb_6(\mu_3\text{-}OH)_8(L)_6(H_2O)_6]$ **32**	H_2L = 2-hydroxyterephthalic acid	159
Asp	$[[Tb(\mu_6\text{-}H_2L)(\mu_2\text{-}OH_2)_2]\cdot xH_2O]_n$ **33**	H_5L = 5,5'-((5-carboxy-1,3-phenylene)-bis(oxy))diisophthalic acid	160
Asp	$\{[(CH_3)_2NH_2]_5[Tb_5(L)_5]\cdot solvent\}_n$ **34**	H_4L = 1,3,5,7-tetra(4-carboxybenzene)pyrene	161
Trp	$[Sm_2(L)_{1.5}(H_2O)_8]\cdot 6H_2O$ **35**	H_4L = 1,2,4,5-benzenetetracarboxylic acid	162
Tyr	$[La(HL)(DMF)_2(NO_3)]$ **36**	H_3L = 5-(4-(tetrazol-5-yl)phenyl)-isophthalic acid	163
DCN	$[Tb_3(HL)(L)(H_2O)_6]\cdot NMP\cdot 3H_2O$ **37**	H_5L = 3,5-di(2′,4′-dicarboxylphenyl)benzoic acid	164
3,5-DCA/3,4-DCA	$Tb^{3+}@\{[NH_2(CH_3)_2]_4\cdot[Cd_6(L)_4(HTz)_{1.5}(H_2O)_6]\cdot xS\}_n$ **38**	H_4L = 3,5-di(2,4-dicarboxylphenyl)pyridine, HTz = 1H-tetrazole	166
temperature	$([(CH_3)_2NH_2]Eu_{0.036}Tb_{0.964}L)$ **39**	H_4L = biphenyl-3,30,5,50-tetracarboxylic acid	60
temperature	$[Yb_{0.05}Nd_{0.95}Cl(L)\cdot(DMF)]$ **40**	H_2L = 2,6-naphthalenedicarboxylic acid	61
humidity	$[DMA]_3[Eu_4L_4\cdot 3DMA\cdot 7H_2O]$ **41**	H_3L = [1,1′-biphenyl]-3,4′,5-tricarboxylic acid	167

Table 2. Comparison of Quenching Coefficient (K_{sv}), Limit of Detection (LOD), Response Time and Sensing Mechanism of Selected Ln-MOFs

Ln-MOFs	Sensing target	Medium	Quenching coefficient (K_{sv}, M^{-1})	Limit of detection (LOD, M)	Response	Sensing mechanism	Refs.
1	Fe^{3+}	H_2O	3.50×10^3	138.8 ppm	-	competitive absorption and [a]FRET	112
2	Fe^{3+}	H_2O	1.88×10^4	5.70×10^{-7}	10 s	competitive absorption and energy transfer	113
3	Fe^{3+}	DMF	1.62×10^5	3.50×10^{-7}	< 60 s	competitive absorption and electronic interaction	114
4	Cu^{2+}	H_2O	3.95×10^3	3.30×10^{-6}	-	energy absorption and weak coordination interaction	115
5	Cu^{2+}	DMF	4.62×10^3	2.53×10^{-5}	-	weak interaction	116
	Fe^{3+}	DMF	4.84×10^3	1.32×10^{-5}	-	competitive absorption and weak interaction	
6	Cd^{2+}	H_2O	[b]23-fold	-	-	coordination interaction between Cd^{2+} and COOH group	117
8	Hg^{2+}	H_2O	9.11×10^4	1.00×10^{-6}	-	profound interaction between Hg^{2+} and O from COOH	119
9	Mg^{2+}	EtOH	[b]10.4-fold	1.53×10^{-10}	15 s	weak coordination of Mg^{2+} with O atoms in the ligand	120
10	Fe^{3+}	H_2O	6.80×10^3	-	< 40 s	competitive absorption and weak interaction	121
11	Fe^{3+}	$EtOH/H_2O$	1.96×10^3	1.68×10^{-5}	-	competitive absorption and dynamic quenching	122
13	Cu^{2+}	H_2O	4.90×10^6	1.35×10^{-9}	15 s	coordination between the framework and Cu^{2+}	124
14	Cd^{2+}	DMF/H_2O	-	5.0×10^{-7}	-	decomposition of the framework	125
15	$Cr_2O_7^{2-}$	DMF	1.40×10^4	5.6×10^{-6}	< 60 s	competitive absorption	135
16	CrO_4^{2-}	H_2O	1.11×10^4	6.5×10^{-7}	10 s	competitive absorption	136
	$Cr_2O_7^{2-}$	H_2O	1.55×10^4	8.9×10^{-7}	10 s	competitive absorption	

Chin. J. Struct. Chem. **2022**, 41, 2211045-2211070
DOI: 10.14102/j.cnki.0254-5861.2022-0138

17	CrO_4^{2-}	H_2O	1.74×10^3	-	-	competitive absorption and weak interaction	137
	$Cr_2O_7^{2-}$	H_2O	1.36×10^3			competitive absorption and weak interaction	
	MnO_4^-	H_2O	0.51×10^3			competitive absorption and weak interaction	
18	$Cr_2O_7^{2-}$	H_2O	1.05×10^3	8.94×10^{-5}	-	competitive absorption	138
19	MnO_4^-	H_2O	1.20×10^3	4.48×10^{-8}		competitive absorption	
20	MnO_4^-	H_2O	-	1.97×10^{-8}	-	competitive absorption and FRET	139
21	CO_3^{2-}	DMSO	-	[c]1.23×10^{-5}		hydrogen bonding interaction	140
				[d]7.80×10^{-5}		hydrogen bonding interaction	
22	NO_2^-	H_2O	4.74×10^5	2.82×10^{-8}	-	dynamic quenching behaviour	141
23	$C_2O_4^2$	DMA	2.07×10^3	1.65×10^{-5}	-	electrostatic interaction and energy-transfer	142
24	ODZ	H_2O	3.52×10^4	5.20×10^{-7}	-	competitive absorption	150
	NFT	H_2O	2.33×10^4	4.30×10^{-7}		competitive absorption	
25	SOM	H_2O	[e]1.10×10^3	-	10 s	photo-induced electron transfer (PET)	151
	NFT	H_2O	1.90×10^4	4.10×10^{-7}	10 s	PET and competitive absorption	
	DTZ	H_2O	1.00×10^4	1.39×10^{-6}	10 s	PET and competitive absorption	
26	NFT	H_2O	5.29×10^4	9.92×10^{-6}	-	PET	152
	NZF	H_2O	4.38×10^4	1.14×10^{-5}		PET	
27	TCH	H_2O	3.09×10^5	4.88×10^{-6}	-	PET and competitive absorption	153
28	NFZ	H_2O	-	4.76×10^{-8}	-	competitive absorption and PET	154
	FZD	H_2O		4.82×10^{-8}		competitive absorption and PET	
29	NZF	H_2O	5.98×10^4	5.02×10^{-7}	-	PET and inner-filter effect (IFE)	155
	NFT	H_2O	6.69×10^4	4.48×10^{-7}		PET and inner-filter effect (IFE)	
30	NIF	DMF	1.10×10^4	8.10×10^{-5}	-	competitive absorption and collision interaction	156
31	SMZ	H_2O	4.60×10^4	6.55×10^{-7}	-	inner-filter effect (IFE)	157
32	Glu	H_2O	-	3.60×10^{-6}	-	PET	159
33	Asp	H_2O	9.90×10^3	7.95×10^{-6}	-	collision interaction	160
34	Asp	EtOH	-	0.025 ppm	-	energy transfer from Asp to ligand	161
35	Trp	H_2O	-	3.30×10^{-7}	< 60 s	coordination between Trp and Sm^{3+}	162
36	Tyr	EtOH	1.40×10^4	3.60×10^{-6}	-	hydrogen bonding interaction	163
	NFT	EtOH	3.00×10^3	1.70×10^{-5}		hydrogen bonding interaction	
37	DCN	H_2O	6.42×10^4	1.4×10^{-7}	30 s	PET	164
38	3,4-DCA	DMF	25.11 $mL \cdot mg^{-1}$	0.0033 $mg \cdot mL^{-1}$	15 s	IFE at low concentration and dynamic and static quenching at high concentration	166
	3,5-DCA	DMF	30.21 $mL \cdot mg^{-1}$	0.0026 $mg \cdot mL^{-1}$	15 s		
39	temperature	solid-state	[f]9.42% K^{-1}	[g]73.9%	-	-	60
40	temperature	solid-state	[f]0.1 and 0.2% K^{-1}	-	-	-	61
41	humidity	solid-state	-	0.0003% (v/v)	30 s	coordination interaction between open Eu^{3+} sites and H_2O	167

DOI: 10.14102/j.cnki.0254-5861.2022-0138

$^4F_{3/2} \rightarrow {}^4I_{11/2}$ transition at 10666 nm for Nd^{3+} were both increased and the temperature and the luminescent intensity ratio (I_{980}/I_{1066}) were fitted linearly. And the relative sensitivities were varied between approximately 0.1 and 0.2% K^{-1}. All the above discussion revealed that this Yb^{3+}/Nd^{3+}-MOF **40** can be considered as an excellent near-infrared luminescence thermometry with high sensitivity.

Wang et al. prepared a Eu-MOF (**41**) with plentiful weak Eu-O bonds, possibly generating affluent open metal sites (OMSs).[167] Profited from the potential open metal site, water molecules were observed to bind with the open Eu^{3+} sites by X-ray single-crystal diffraction. Luminescent spectrum of **41** excited at 365 nm exhibited two main emission bands: the emission band centered at 439 nm from the ligand and the typical emission peaks of Eu^{3+} located at 593, 617 and 653 nm, indicating that compound **41** possessed a dual-emissive ratiometric luminescence behavior. Thus, the performance of **41** as a ratiometric luminescent probe was explored. Interestingly, as the relative humidity (RH) of the air gradually increased from ~0% to ~40%, the luminescent intensity at 617 nm decreased obviously, while that at 439 nm was found to increase continuously, leading to the luminescence color changing gradually from red to blue-purple, revealing that compound **41** can act as a ratiometric luminescent sensor for humidity by naked eyes.

n CONCLUSION AND OUTLOOK

The purposes of this review are aimed to make a classification and summary for recent researches of Ln-MOFs as chemical sensors for ions, antibiotics and amino acids based on “turn on” or “turn off” effects (Table 1), especially the applications of water-stable Ln-MOFs, as well as the probable sensing mechanism. With the continuous development of industry and agriculture, pollutants discharged from industry, agriculture, and daily life to environment have accentuated burden on the environment and became hidden threats to the health of humans, which can enter to the organism through bio-enrichment. In recent years, great and numerous efforts have been executed on the exploration for the efficient methods and materials to detecting environmental pollutions or vital substances of human body. Compared with other detection methods or materials, it is well known that luminescent sensors based on lanthanide metal-organic frameworks (Ln-MOFs) have emerging, benefited from their incomparable advantages of structural diversity, typical emissions and easy operation. Up to now, tens of thousands of Ln-MOFs have been meticulously designed and exploited, and can be applied as luminescent probers for varieties of analytes, such as metal cations, anions, antibiotics, biomarkers, amino acids, and so on.

In order to improve the abilities of luminescent chemical sensors in practical application, developing Ln-MOFs with high stability in water, outlet water or human urine is still a huge challenge since stability is the first step for luminescent sensors towards practical application. On the other hand, the performance for many reported luminescent sensors has been just investigated in aqueous solutions, unable to demonstrate the potential for practical application. Thus, the detection capacity of developed Ln-MOFs in outlet water, domestic water and human serum or urine should be researched as an important project. Besides, for fast, convenient and real-time detection, more attention is deserved to focus on the exploitation of diverse functionalized Ln-MOFs devices, such as luminescent test papers, Ln-MOFs thin films and luminescent encodes. In addition, some other issues, such as the stability of the sensing performance, the sensing mechanism and the relationship between structural features and luminescent properties, are still challenging problems needed to be solved in practical application of luminescent sensors based on Ln-MOFs materials. As we know, Ln^{3+} ions are inclined to coordinate with the oxygen atoms from carboxylate groups. Therefore, ligands with multi-carboxylate groups and large conjugated systems can improve the coordinated numbers of lanthanide ions and reduce the presence of H_2O molecules in the coordination sphere, making the structures stable. That is, introducing ligands with abundant coordinated sites is beneficial to heighten the stability of Ln-MOFs and broad their application in practical conditions. Besides, ligands with well-matched triplet energy with central Ln^{3+} ion can efficiently sensitize Ln^{3+} through “antenna effect”, thus making the design of high luminescent Ln-MOFs reliable. As a consequence, more efforts should continue to be made on the functionalized design and synthesis of Ln-MOFs.

n ACKNOWLEDGEMENTS

This work was financially supported by the National Natural Science Foundation of China (21801107), the Natural Science Foundation of Shandong Province (ZR2018BB005), and the Youth Innovation Team of Shandong Colleges and Universities (2019KJC027).

n AUTHOR INFORMATION

Corresponding authors. Emails: yangyan@lcu.edu.cn and cl@fjirsm.ac.cn

n COMPETING INTERESTS

The authors declare no competing interests.

n ADDITIONAL INFORMATION

Full paper can be accessed via
http://manu30.magtech.com.cn/jghx/EN/10.14102/j.cnki.0254-5861.2022-0138
For submission: https://www.editorialmanager.com/cjschem

n REFERENCES

(1) Yuan, H. Y.; Li, N. X.; Fan, W. D.; Cai, H.; Zhao, D. Metal-organic framework based gas sensors. *Adv. Sci.* **2022**, 9, 2104374.

(2) Pal, S.; Yu, S. S.; Kung, C. W. Group 4 metal-based metal-organic frameworks for chemical sensors. *Chemosensors* **2021**, 9, 306.

(3) Morozova, S. M.; Sharsheeva, A.; Morozov, M. I.; Vinogradov, A. V.; Hey-Hawkins, E. Bioresponsive metal-organic frameworks: rational design and function. *Coord. Chem. Rev.* **2021**, 431, 213682.

(4) Jin, J.; Xue, J. J.; Liu, Y. C.; Yang, G. P.; Wang, Y. Y. Recent progresses in luminescent metal-organic frameworks (LMOFs) as sensors for the detection of anions and cations in aqueous solution. *Dalton Trans.* **2021**, 50, 1950-1972.

(5) Zhang, Y. M.; Yuan, S.; Day, G.; Wang, X.; Yang, X. Y.; Zhou, H. C. Luminescent sensors based on metal-organic frameworks. *Coord. Chem. Rev.* **2018**, 354, 28-45.
(6) Razavi, S. A. A.; Morsali, A. Metal ion detection using luminescent-MOFs: principles, strategies and roadmap. *Coord. Chem. Rev.* **2020**, 415, 213299.
(7) Ghasempour, H.; Wang, K. Y.; Powell, J. A.; ZareKarizi, F.; Lv, X. L.; Morsali, A.; Zhou, H. C. Metal-organic frameworks based on multicarboxylate linkers. *Coord. Chem. Rev.* **2021**, 426, 213542.
(8) Shu, Y.; Ye, Q.; Dai, T.; Xu, Q.; Hu, X. Encapsulation of luminescent guests to construct luminescent metal-organic frameworks for chemical sensing. *ACS Sensors* **2021**, 6, 641-658.
(9) Liu, J. Q.; Luo, Z. D.; Pan, Y.; Kumar Singh, A.; Trivedi, M.; Kumar, A. Recent developments in luminescent coordination polymers: designing strategies, sensing application and theoretical evidences. *Coord. Chem. Rev.* **2020**, 406, 213145.
(10) Wang, Y. L.; Li, X. Y.; Han, S. D.; Pan, J.; Xue, Z. Z. A Cu_2I_2-based coordination framework as the selective sensor for Ag^+ and the effective adsorbent for I_2. *Cryst. Growth Des.* **2022**, 10.1021/acs.cgd.2c00080.
(11) Xiong, K. C.; Li, X.; Shi, Y. W.; Zhang, J. L.; Zhang, Y.; Zhang, K. H.; Wu, M. Y.; Gai, Y. L. Sodalite Cd_{66}-cage-based metal-organic framework constructed by Cd_9 and Cd_5 metal-organic clusters. *Inorg. Chem.* **2021**, 60, 17435-17439.
(12) Pang, J. D.; Di, Z. Y.; Qin, J. S.; Yuan, S.; Lollar, T. C.; Li, J. L.; Zhang, P.; Wu, M. Y.; Yuan, D. Q.; Hong, M. C.; Zhou, H. C. Precisely embedding active sites into a mesoporous Zr-framework through linker installation for high-efficiency photocatalysis. *J. Am. Chem. Soc.* **2020**, 142, 15020-15026.
(13) Zhu, S. Y.; Zhao, L. M.; Yan. B. A novel spectroscopic probe for detecting food preservative NO_2^-: citric acid functionalized metal-organic framework and luminescence sensing. *Microchem. J.* **2020**, 155, 104768.
(14) Li, Y. W.; Li, J.; Wan, X. Y.; Sheng, D. F.; Yan, H.; Zhang, S. S.; Ma, H. Y.; Wang, S. N.; Li, D. C.; Gao, Z. Y.; Dou, J. M.; Sun, D. Nanocage-based N-rich metal-organic framework for luminescence sensing toward Fe^{3+} and Cu^{2+} Ions. *Inorg. Chem.* **2021**, 60, 671-681.
(15) Xian, G. X.; Wang, L. Y.; Wan, X. Y.; Yan, H.; Cheng, J. W.; Chen, Y. Q.; Lu, J.; Li, Y. W.; Li, D. C.; Dou, J. M.; Wang, S. N. Two multiresponsive luminescent Zn-MOFs for the detection of different chemicals in simulated urine and antibiotics/cations/anions in aqueous media. *Inorg. Chem.* **2022**, 61, 7238-7250.
(16) Sun, T. Y.; Gao, Y. B.; Du, Y. Y.; Zhou, L.; Chen, X. Recent advances in developing lanthanide metal-organic frameworks for ratiometric fluorescent sensing. *Front. Chem.* **2020**, 8, 624592.
(17) Younis, S. A.; Bhardwaj, N.; Bhardwaj, S. K.; Kim, K. H.; Deep, A. Rare earth metal-organic frameworks (RE-MOFs): synthesis, properties, and biomedical applications. *Coord. Chem. Rev.* **2021**, 429, 213620.
(18) Belousov, Y. A.; Drozdov, A. A.; Taydakov, I. V.; Marchetti, F.; Pettinari, R.; Pettinari, C. Lanthanide azolecarboxylate compounds: structure, luminescent properties and applications. *Coord. Chem. Rev.* **2021**, 445, 214084.
(19) Chen, X.; Xu, Y.; Li, H. R. Lanthanide organic/inorganic hybrid systems: efficient sensors for fluorescence detection. *Dyes Pigm.* **2020**, 178, 108386.
(20) Armelao, L.; Quici, S.; Barigelletti, F.; Accorsi, G.; Bottaro, G.; Cavazzini, M.; Tondello, E. Design of luminescent lanthanide complexes: from molecules to highly efficient photo-emitting materials. *Coord. Chem. Rev.* **2010**, 254, 487-505.
(21) Li, B.; Wen, H. M.; Cui, Y. J.; Qian, G. D.; Chen, B. L. Multifunctional lanthanide coordination polymers. *Prog. Polym. Sci.* **2015**, 48, 40-84.
(22) Yi, F. Y.; Chen, D. X.; Wu, M. K.; Han, L.; Jiang, H. L. Chemical sensors based on metal organic frameworks. *ChemPlusChem* **2016**, 81, 675-690.
(23) Fan, T. N.; Xia, T. F.; Zhang, Q.; Cui, Y. J.; Yang, Y.; Qian, G. D. A porous and luminescent metal-organic framework containing triazine group for sensing and imaging of Zn^{2+}. *Micropor. Mesopor. Mat.* **2018**, 266, 1-6.
(24) Wu, C. M.; Feng, Z. H.; Zhou, H. Q.; Yu, F. Y.; Li, J. R.; Ye, X. H.; Hu, J. Y.; Chung, L. H.; Liao, W. M.; He, J. Metal-organic frameworks constructed from trivalent lanthanide nodes (Eu^{3+}, Tb^{3+}, and Dy^{3+}) and thiophenethio-functionalized linker with photoluminescent response selective towards Ag^+ ions. *Dyes Pigm.* **2022**, 198, 109999.
(25) Yang, Y.; Jiang, F. L.; Chen, L.; Pang, J. D.; Wu, M. Y.; Wan, X. Y.; Pan, J.; Qian, J. J.; Hong, M. C. An unusual bifunctional Tb-MOF for highly sensitive sensing of Ba^{2+} ions and with remarkable selectivities for CO_2-N_2 and CO_2-CH_4. *J. Mater. Chem. A* **2015**, 3, 13526-13532.
(26) Wu, N.; Guo, H.; Wang, X. Q.; Sun, L.; Zhang, T. T.; Peng, L. P.; Yang, W. A water-stable lanthanide-MOF as a highly sensitive and selective luminescence sensor for detection of Fe^{3+} and benzaldehyde. *Colloids Surf. A: Physicochem. Eng. Aspects* **2021**, 616, 126093.
(27) Jia, P.; Wang, Z. H.; Zhang, Y. F.; Zhang, D.; Gao, W. C.; Su, Y.; Li, Y. B.; Yang, C. L. Selective sensing of Fe^{3+} ions in aqueous solution by a biodegradable platform based lanthanide metal organic framework. *Spectrochim. Acta, Part A: Mol. Biomol. Spectrosc*. **2020**, 230, 118084.
(28) Xiao, X. F.; Ren, L. P.; Wang, S. J.; Zhang, Q.; Zhang, Y. W.; Liu, R. N.; Xu, W. L. Controllable production of micro-nanoscale metal-organic frameworks coatings on cotton fabric for sensing Cu^{2+}. *Fiber. Polym.* **2020**, 21, 2003-2009.
(29) Wang, W. B.; Wang, R. Y.; Ge, Y. F.; Wu, B. L. Color tuning and white light emission by codoping in isostructural homochiral lanthanidmetal-organic frameworks. *RSC Adv.* **2018**, 8, 42100-42108.
(30) Li, J. X.; Guan, Q. L.; You, Z. X.; Wang, Y.; Shi, Z.; Xing, Y. H.; Bai, F. Y.; Sun, L. X. Achieving multifunctional detection of Th^{4+} and UO_2^{2+} in the post-synthetically modified metal-organic framework and application of functional MOF membrane. *Adv. Mater. Technol.* **2021**, 6, 2001184.
(31) Song, X. Q.; Meng, H. H.; Lin, Z. G.; Wang, L. 2D lanthanide coordination polymers: synthesis, structure, luminescent properties, and ratiometric sensing application in the hydrostable PMMA-doped hybrid films. *ACS Appl. Polym. Mater.* **2020**, 2, 1644-1655.
(32) Chen, X. L.; Shang, L.; Liu, L.; Yang, H.; Cui, H. L.; Wang, J. J. A highly sensitive and multi-responsive Tb-MOF fluorescent sensor for the detection of Pb^{2+}, $Cr_2O_7^{2-}$, $B_4O_7^{2-}$, aniline, nitrobenzene and cefixime. *Dyes Pigm.* **2021**, 196, 109809.
(33) Mandal, T. N.; Karmakar, A.; Sharma, S.; Ghosh, S. K. Metal-organic frameworks (MOFs) as functional supramolecular architectures for anion recognition and sensing. *Chem. Rec.* **2018**, 18, 154-164.
(34) Guo, H.; Wu, N.; Xue, R.; Liu, H.; Wang, M. Y.; Yao, W. Q.; Wang, X. Q.; Yang, W. An Eu(III)-functionalized Sr-based metal-organic framework for fluorometric determination of Cr(III) and Cr(VI) ions. *Microchimica Acta* **2020**, 187, 374.
(35) Zhang, P. F.; Yang, G. P.; Li, G. P.; Yang, F.; Liu, W. N.; Li, J. Y.; Wang, Y. Y. Series of water-stable lanthanide metal-organic frameworks based on carboxylic acid imidazolium chloride: tunable luminescent

DOI: 10.14102/j.cnki.0254-5861.2022-0138

emission and sensing. *Inorg. Chem.* **2019**, 58, 13969-13978.

(36) Tan, G.; Jia, R. Q.; Wu, W. L.; Li, B.; Wang, L. Y. Highly pH-stable Ln-MOFs as sensitive and recyclable multifunctional materials: luminescent probe, tunable luminescent, and photocatalytic performance. *Cryst. Growth Des.* **2021**, 22, 323-333.

(37) Das, A.; Das, S.; Trivedi, V.; Biswas, S. A dual functional MOF-based fluorescent sensor for intracellular phosphate and extracellular 4-nitrobenzaldehyde. *Dalton Trans.* **2019**, 48, 1332-1343.

(38) Wang, J. Y.; Li, W. Y.; Zheng, Y. Q. Colorimetric assay for the sensitive detection of phosphate in water based on metal-organic framework nanospheres possessing catalytic activity. *New J. Chem.* **2020**, 44, 19683-19689.

(39) Yin, J.; Chu, H. T.; Qin, S. L.; Qi, H. Y.; Hu, M. G. Preparation of $Eu_{0.075}Tb_{0.925}$-metal organic framework as a fluorescent probe and application in the detection of Fe^{3+} and $Cr_2O_7^{2-}$. *Sensors* **2021**, 21, 7355.

(40) Zhang, G. S.; Wu, G. H.; Zhang, H.; Wang, G. N.; Han, H. T. A stable terbium(III) metal-organic framework as a dual luminescent sensor for MnO_4^- ions and nitroaromatic explosives. *J. Solid State Chem.* **2021**, 295, 121924.

(41) Gao, W.; Zhou, A. M.; Wei, H.; Wang, C. L.; Liu, J. P.; Zhang, X. M. Water-stable Ln^{III}-based coordination polymers displaying slow magnetic relaxation and luminescence sensing properties. *New J. Chem.* **2020**, 44, 6747-6759.

(42) Yin, S. Y.; Fu, P. Y.; Pan, M.; Guo, J.; Fan, Y. N.; Su, C. Y. Reverse photoluminescence responses of Ln(III) complexes to methanol vapor clarify the differentiated energy transfer pathway and potential for methanol detection and encryption. *J. Mater. Chem. C* **2020**, 8, 16907-16914.

(43) Ren, J. Y.; Niu, Z.; Ye, Y. X.; Tsai, C. Y.; Liu, S. X.; Liu, Q. Z.; Huang, X. Q.; Zafady, A.; Ma, S. Q. Second-sphere interaction promoted turn-on fluorescence for selective sensing of organic amines in a Tb^{III}-based macrocyclic framework. *Angew. Chem. Int. Ed.* **2021**, 60, 23705-23712.

(44) Feng, L.; Dong, C. L.; Li, M. F.; Li, L. X.; Jiang, X.; Gao, R.; Wang, R. J.; Zhang, L. J.; Ning, Z. L.; Gao, D. J.; Bi, J. Terbium-based metal-organic frameworks: highly selective and fast respond sensor for styrene detection and construction of molecular logic gate. *J. Hazard. Mater.* **2020**, 388, 121816.

(45) Yang, Y.; Li, L. Z.; Yang, H.; Sun, L. Five lanthanide-based metal-organic frameworks built from a π-conjugated ligand with isophthalate units featuring sensitive fluorescent sensing for DMF and acetone molecules. *Cryst. Growth Des.* **2021**, 21, 2954-2961.

(46) Wang, C. L.; Zheng, Y. X.; Chen, L.; Zhu, C. Y.; Gao, W.; Li, P.; Liu, J. P.; Zhang, X. M. The construction of a multifunctional luminescent Eu-MOF for the sensing of Fe^{3+}, $Cr_2O_7^{2-}$ and amines in aqueous solution. *CrystEngComm* **2021**, 23, 7581-7589.

(47) Wang, H. F.; Ma, X. F.; Zhu, Z. H.; Zou, H. H.; Liang, F. P. Regulation of the metal center and coordinating anion of mononuclear Ln(III) complexes to promote an efficient luminescence response to various organic solvents. *Langmuir* **2020**, 36, 1409-1417.

(48) Wang, H. F.; Zhu, Z. H.; Peng, J. M.; Yin, B.; Wang, H. L.; Zou, H. H.; Liang, F. P. Multifunctional binuclear Ln(III) complexes obtained *via* in situ tandem reactions: multiple photoresponses to volatile organic solvents and anticounterfeiting and magnetic properties. *Inorg. Chem.* **2020**, 59, 13774-13783.

(49) Zeng, X. L.; Long, Z.; Jiang, X. F.; Zhang, Y. J.; Liu, Q.; Hu, J.; Li, C. H.; Wu, L.; Hou, X. D. Single bimetallic lanthanide-based metal-organic frameworks for visual decoding of a broad spectrum of molecules. *Anal. Chem.* **2020**, 92, 5500-5508.

(50) Guo, H. D.; Wang, F. Y.; Ma, R. D.; Zhang, M.; Fu, L. S.; Zhou, T.; Liu, S.; Guo, X. M. Lanthanide post-functionalized UiO-67 type metal-organic frameworks for tunable light-emission and stable multi-sensors in aqueous media. *Inorg. Chim. Acta* **2021**, 518, 120229.

(51) Zhan, C. H.; Huang, D. P.; Wang, Y.; Mao, W. T.; Wang, X. J.; Jiang, Z. G.; Feng, Y. L. Four anionic Ln-MOFs for remarkable separation of C_2H_2-CH_4/CO_2-CH_4 and highly sensitive sensing of nitrobenzene. *CrystEngComm* **2021**, 23, 2788-2792.

(52) Ma, L. L.; Yang, G. P.; Li, G. P.; Zhang, P. F.; Jin, J.; Wang, Y.; Wang, J. M.; Wang, Y. Y. Luminescence modulation, near white light emission, selective luminescence sensing, and anticounterfeiting *via* a series of Ln-MOFs with a π-conjugated and uncoordinated Lewis basic triazolyl ligand. *Inorg. Chem. Front.* **2021**, 8, 329-338.

(53) Liu, W. S.; Li, D. P.; Wang, F.; Chen, X. Y.; Wang, X. Q.; Tian, Y. A luminescent lanthanide MOF as highly selective and sensitive fluorescent probe for nitrobenzene and Fe^{3+}. *Opt. Mater.* **2022**, 123, 111895.

(54) Wang, M.; Gao, H. W.; Li, J. X.; Bai, F. Y.; Xing, Y. H.; Shi, Z. Multifuntional luminescence sensing and white light adjustment of lanthanide metal-organic frameworks constructed from the flexible cyclotriphosphazene-derived hexacarboxylic acid ligand. *Dalton Trans.* **2021**, 50, 14618-14628.

(55) Lin, Z. G.; Song, F. Q.; Wang, H.; Song, X. Q.; Yu, X. X.; Liu, W. S. The construction of a novel luminescent lanthanide framework for the selective sensing of Cu^{2+} and 4-nitrophenol in water. *Dalton Trans.* **2021**, 50, 1874-1886.

(56) Zhou, T.; Liu, S.; Wang, S.; Mi, S. Y.; Gao, P.; Guo, X. M.; Su, Q. J.; Guo, H. D. Dual-function lanthanide-organic frameworks based on a zwitterionic ligand as a ratiometric thermometer and a selective sensor for nitroaromatic explosives. *Ind. Eng. Chem. Res.* **2021**, 60, 11760-11767.

(57) Wang, J. M.; Zhang, P. F.; Cheng, J. G.; Wang, Y.; Ma, L. L.; Yang, G. P.; Wang, Y. Y. Luminescence tuning and sensing properties of stable 2D lanthanide metal-organic frameworks built with symmetrical flexible tricarboxylic acid ligands containing ether oxygen bonds. *CrystEngComm* **2021**, 23, 411-418.

(58) Wang, Q. Q.; Guo, Z. H.; Zhang, Y. D.; Ma, L. L.; Zhang, P. F.; Yang, G. P.; Wang, Y. Y. White light emission phosphor modulation, nitrobenzene sensing property and barcode anti-counterfeiting *via* lanthanides post-functionalized metal-organic frameworks. *J. Solid State Chem.* **2022**, 307, 122854.

(59) Deng, L. M.; Zhao, H. H.; Liu, K.; Ma, D. X. Efficient luminescence sensing in two lanthanide metal-organic frameworks with rich uncoordinated Lewis basic sites. *CrystEngComm* **2021**, 23, 6591-6598.

(60) Pan, Y.; Su, H. Q.; Zhou, E. L.; Yin, H. Z.; Shao, K. Z.; Su, Z. M. A stable mixed lanthanide metal-organic framework for highly sensitive thermometry. *Dalton Trans.* **2019**, 48, 3723-3729.

(61) Gomez, G. E.; Marin, R.; Carneiro Neto, A. N.; Botas, A. M. P.; Ovens, J.; Kitos, A. A.; Bernini, M. C.; Carlos, L. D.; Soler-Illia, G. J. A. A.; Murugesu, M. Tunable energy-transfer process in heterometallic MOF materials based on 2,6-naphthalenedicarboxylate: solid-state lighting and near-infrared luminescence thermometry. *Chem. Mater.* **2020**, 32, 7458-7468.

(62) Feng, T. T.; Ye, Y. X.; Liu, X.; Cui, H.; Li, Z. Q.; Zhang, Y.; Liang, B.; Li, H. R.; Chen, B. L. A robust mixed-lanthanide polyMOF membrane for ratiometric temperature sensing. *Angew. Chem. Int. Ed.* **2020**, 59, 21752-21757.

DOI: 10.14102/j.cnki.0254-5861.2022-0138

(63) Liu, W.; Zhao, M. Y.; Xiang, G. T.; Han, Z. L.; Xia, F.; Wang, J. W. High-efficiency energy transfer pathways between Er(III) and Tm(III) in metal-organic frameworks for tunable upconversion emission and optical temperature sensing. *J. Lumin.* **2021**, 239, 118296.
(64) McLaurin, E. J.; Bradshaw, L. R.; Gamelin, D. R. Dual-emitting nanoscale temperature sensors. *Chem. Mater.* **2013**, 25, 1283-1292.
(65) Yu, W. T.; Chen, H. B.; Wu, H. J.; Lin, P. C.; Xu, H. H.; Xie, Q. W.; Shi, K. Z.; Xie, G. X.; Chen, Y. Continuous-flow rapid synthesis of wavelength-tunable luminescent lanthanide metal-organic framework nanorods by a microfluidic reactor. *J. Alloys Compd.* **2022**, 890, 161860.
(66) Li, Y. P.; Xiao, X. Y.; Wei, Z.; Chen, Y. A ratio fluorescence thermometer based on carbon dots & lanthanide functionalized metal-organic frameworks. *Z. Anorg. Allg. Chem.* **2022**, e202100323.
(67) Yuan, R. R.; He, H. M. State of the art methods and challenges of luminescent metal-organic frameworks for antibiotic detection. *Inorg. Chem. Front.* **2020**, 7, 4293-4319.
(68) Yang, H. W.; Xu, P.; Ding, B.; Liu, Z. Y.; Zhao, X. J.; Yang, E. C. A highly stable luminescent Eu-MOF exhibiting efficient response to nitrofuran antibiotics through the inner filter effect and photoinduced electron transfer. *Eur. J. Inorg. Chem.* **2019**, 2019, 5077-5084.
(69) Li, J. M.; Huo, R.; Li, X.; Sun, H. L. Lanthanide-organic frameworks constructed from 2,7-naphthalenedisulfonate and 1H-imidazo[4,5-f][1,10]-phenanthroline: synthesis, structure, and luminescence with near-visible light excitation and magnetic properties. *Inorg. Chem.* **2019**, 58, 9855-9865.
(70) Lei, M. Y.; Wang, X. H.; Zhang, T. J.; Shi, Y.; Wen, J. H.; Zhang, Q. F. Homochiral Eu^{3+}@MOF composite for the enantioselective detection and separation of (R/S)-ornidazole. *Inorg. Chem.* **2022**, 61, 6764-6772.
(71) Yang, Y.; Zhao, L. N.; Sun, M. A.; Wei, P. P.; Li, G. M.; Li, Y. X. Highly sensitive luminescent detection toward polytypic antibiotics by a water-stable and white-light-emitting MOF-76 derivative. *Dyes and Pigments* **2020**, 180, 108444.
(72) Liu, D. M.; Dong, G. Y.; Wang, X.; Nie, F. M.; Li, X. A luminescent Eu coordination polymer with near-visible excitation for sensing and its homologues constructed from 1,4-benzenedicarboxylate and 1H-imidazo-[4,5-f][1,10]-phenanthroline. *CrystEngComm* **2020**, 22, 7877-7887.
(73) Sun, T. C.; Fan, R. Q.; Xiao, R.; Xing, T. F.; Qin, M. Y.; Liu, Y. Q.; Hao, S.; Chen, W.; Yang, Y. L. Anionic Ln-MOF with tunable emission. *J. Mater. Chem. A* **2020**, 8, 5587-5594.
(74) Wang, X. R.; Huang, Z.; Du, J.; Wang, X. Z.; Gu, N.; Tian, X.; Li, Y.; Liu, Y. Y.; Huo, J. Z.; Ding, B. Hydrothermal preparation of five rare-earth (Re = Dy, Gd, Ho, Pr, and Sm) luminescent cluster-based coordination materials: the first MOFs-based ratiometric fluorescent sensor for lysine and bifunctional sensing platform for insulin and Al^{3+}. *Inorg. Chem.* **2018**, 57, 12885-12899.
(75) Sun, Y. X.; Guo, G.; Ding, W. M.; Han, W. Y.; Li, J.; Deng, Z. P. A highly stable Eu-MOF multifunctional luminescent sensor for the effective detection of Fe^{3+}, $Cr_2O_7^{2-}$/CrO_4^{2-} and aspartic acid in aqueous systems. *CrystEngComm* **2022**, 24, 1358-1367.
(76) Han, L. J.; Kong, Y. J.; Hou, G. Z.; Chen, H. C.; Zhang, X. M.; Zheng, H. G. A europium-based MOF fluorescent probe for efficiently detecting malachite green and uric acid. *Inorg. Chem.* **2020**, 59, 7181-7187.
(77) Yang, Y.; Pang, J. D.; Li, Y. W.; Sun, L.; Zhang, H.; Zhang, L. X.; Xu, S. T.; Jiang, T. W. Fabrication of a stable europium-based luminescent sensor for fast detection of urinary 1-hydroxypyrene constructed from a tetracarboxylate ligand. *Inorg. Chem.* **2021**, 60, 19189-19196.
(78) Zhang, Y.; Xu, X.; Yan, B. A multicolor-switchable fluorescent lanthanide MOFs triggered by anti-cancer drugs: multifunctional platform for anti-cancer drug sensing and information anticounterfeiting. *J. Mater. Chem. C* **2022**, 10, 3576-3584.
(79) Yu, H. H.; Liu, Q.; Li, J.; Su, Z. M.; Li, X.; Wang, X. L.; Sun, J.; Zhou, C.; Hu, X. L. A dual-emitting mixed-lanthanide MOF with high water-stability for ratiometric fluorescence sensing of Fe^{3+} and ascorbic acid. *J. Mater. Chem. C* **2021**, 9, 562-568.
(80) Cao, W. Q.; Xia, T. F.; Cui, Y. J.; Yu, Y.; Qian, G. D. Lanthanide metal-organic frameworks with nitrogen functional sites for the highly selective and sensitive detection of NADPH. *Chem. Commun.* **2020**, 56, 10851-10854.
(81) Othong, J.; Boonmak, J.; Kielar, F.; Hadsadee, S.; Jungsuttiwong, S.; Youngme, S. Self-calibrating sensor with logic gate operation for anthrax biomarker based on nanoscaled bimetallic lanthanoid MOF. *Sens. Actuators, B: Chem.* **2020**, 316, 128156.
(82) Xia, C.; Xu, Y.; Cao, M. M.; Liu, Y. P.; Xia, J. F.; Jiang, D. Y.; Zhou, G. H.; Xie, R. J.; Zhang, D. F.; Li, H. L. A selective and sensitive fluorescent probe for bilirubin in human serum based on europium(III) post-functionalized Zr(IV)-based MOFs. *Talanta* **2020**, 212, 120795.
(83) Zhou, Y. N.; Liu, L. L.; Liu, Q. W.; Liu, X. X.; Feng, M. Z.; Wang, L.; Sun, Z. G.; Zhu, Y. Y.; Zhang, X.; Jiao, C. Q. Dual-functional metal-organic framework for luminescent detection of carcinoid biomarkers and high proton conduction. *Inorg. Chem.* **2021**, 60, 17303-17314.
(84) Zhao, P. R.; Liu, Y. Q.; He, C.; Duan, C. Y. Synthesis of a lanthanide metal-organic framework and its fluorescent detection for phosphate group-based molecules such as adenosine triphosphate. *Inorg. Chem.* **2022**, 61, 3132-3140.
(85) Shen, M. L.; Liu, B.; Xu, L.; Jiao, H. Ratiometric fluorescence detection of anthrax biomarker 2,6-dipicolinic acid using hetero MOF sensors through ligand regulation. *J. Mater. Chem. C* **2020**, 8, 4392-4400.
(86) Zhou, Z. D.; Wang, C. Y.; Zhu, G. S.; Du, B.; Yu, B. Y.; Wang, C. C. Water-stable europium(III) and terbium(III)-metal organic frameworks as fluorescent sensors to detect ions, antibiotics and pesticides in aqueous solutions. *J. Mol. Struct.* **2022**, 1251, 132009.
(87) Bünzli, J. C. G.; Piguet, C. Taking advantage of luminescent lanthanide ions. *Chem. Soc. Rev.* **2005**, 34, 1048.
(88) Zhang, X. J.; Wang, W. J.; Hu, Z. J.; Wang, G. N.; Uvdal, K. Coordination polymers for energy transfer: preparations, properties, sensing applications, and perspectives. *Coord. Chem. Rev.* **2015**, 284, 206-235.
(89) Sabbatini, N.; Guardigli, M. Luminescent lanthanide complexes as photochemical supramolecular devices. *Coord. Chem. Rev.* **1993**, 123, 201-228.
(90) Kim, H. J.; Lee, J. E.; Kim, Y. S.; Park, N. G. Ligand effect on the electroluminescence mechanism in lanthanide(III) complexes. *Opt. Mater.* **2002**, 21, 181-186.
(91) Cui, Y. J.; Yue, Y. F.; Qian, G. D.; Chen, B. L. Luminescent functional metal-organic frameworks. *Chem. Rev.* **2012**, 112, 1126-1162.
(92) Zhao, Y. F.; Li, D. Lanthanide-functionalized metal-organic frameworks as ratiometric luminescent sensors. *J. Mater. Chem. C* **2020**, 8, 12739-12754.
(93) Cui, Y. J.; Chen, B. L.; Qian, G. D. Lanthanide metal-organic frameworks for luminescent sensing and light-emitting applications. *Coord. Chem. Rev.* **2014**, 273-274, 76-86.
(94) Mahata, P.; Mondal, S. K.; Singha, D. K.; Majee, P. Luminescent rare-earth-based MOFs as optical sensors. *Dalton Trans.* **2017**, 46, 301-

DOI: 10.14102/j.cnki.0254-5861.2022-0138

328.
(95) Yan, B. Luminescence response mode and chemical sensing mechanism for lanthanide-functionalized metal-organic framework hybrids. *Inorg. Chem. Front.* **2021**, 8, 201-233.
(96) Firmino, A. D. G.; Figueira, F.; Tomé, J. P. C.; Paz, F. A. A.; Rocha, J. Metal-organic frameworks assembled from tetraphosphonic ligands and lanthanides. *Coord. Chem. Rev.* **2018**, 355, 133-149.
(97) Zhao, S. N.; Wang, G. B.; Poelman, D.; Voort, P. V. D. Luminescent lanthanide MOFs: a unique platform for chemical sensing. *Materials* **2018**, 11, 572.
(98) Li, X. J.; Lu, S.; Tu, D. T.; Zheng, W.; Chen, X. Y. Luminescent lanthanide metal-organic framework nanoprobes: from fundamentals to bioapplications. *Nanoscale* **2020**, 12, 15021-15035.
(99) Yan, B. Lanthanide-functionalized metal-organic framework hybrid systems to create multiple luminescent centers for chemical sensing. *Acc. Chem. Res.* **2017**, 50, 2789-2798.
(100) Afzal, S.; Maitra, U. Sensitized lanthanide photoluminescence based sensors-a review. *Helv. Chim. Acta* **2022**, 105, e202100194.
(101) Li, B.; Zhao, D. S.; Wang, F.; Zhang, X. X.; Li, W. Q.; Fan, L. M. Recent advances in molecular logic gate chemosensors based on luminescent metal organic frameworks. *Dalton Trans.* **2021**, 50, 14967-14977.
(102) Gorai, T.; Schmitt, W.; Gunnlaugsson, T. Highlights of the development and application of luminescent lanthanide based coordination polymers, MOFs and functional nanomaterials. *Dalton Trans.* **2021**, 50, 770-784.
(103) Liang, G. M.; Wang, S.; Xu, M. Y.; Chen, H. L.; Liang, G. Y.; Gui, L. C.; Wang, X. J. 2D lanthanide coordination polymers constructed from a semi-rigid tricarboxylic acid ligand: crystal structure, luminescence sensing and color tuning. *CrystEngComm* **2020**, 22, 6161-6169.
(104) Shi, Y. W.; Ye, J. W.; Qi, Y.; Akram, M. A.; Rauf, A.; Ning, G. L. An anionic layered europium(III) coordination polymer for solvent-dependent selective luminescence sensing of Fe^{3+} and Cu^{2+} ions and latent fingerprint detection. *Dalton Trans.* **2018**, 47, 17479-17485.
(105) Yuan, M.; Tang, Q.; Lu, Y.; Zhang, Z.; Li, X. H.; Liu, S. M.; Sun, X. W.; Liu, S. X. Using the luminescence and ion sensing experiment of a lanthanide metal-organic framework to deepen and extend undergraduates' understanding of the antenna effect. *J. Chem. Educ.* **2019**, 96, 1256-1261.
(106) Xu, Q. W.; Dong, G. Y.; Cui, R. F.; Li, X. 3D lanthanide-coordination frameworks constructed by a ternary mixed-ligand: crystal structure, luminescence and luminescence sensing. *CrystEngComm* **2020**, 22, 740-750.
(107) Li, H. H.; Han, Y. B.; Shao, Z. C.; Li, N.; Huang, C.; Hou, H. W. Water-stable Eu-MOF fluorescent sensors for trivalent metal ions and nitrobenzene. *Dalton Trans.* **2017**, 46, 12201-12208.
(108) Puglisi, R.; Pellegrino, A. L.; Fiorenza, R.; Scirè, S.; Malandrino, G. A facile one-pot approach to the synthesis of Gd-Eu based metal-organic frameworks and applications to sensing of Fe^{3+} and $Cr_2O_7^{2-}$ ions. *Sensors* **2021**, 21, 1679.
(109) Gomez, G. E.; Afonso, M. D. S.; Baldoni, H. A.; Roncaroli, F.; Soler-Illia, G. J. A. A. Luminescent lanthanide metal organic frameworks as chemosensing platforms towards agrochemicals and cations. *Sensors* **2019**, 19, 1260.
(110) Chen, M.; Wu, K. Y.; Pan, W. L.; Huang, N. H.; Li, R. T.; Chen, J. X. Selective and recyclable tandem sensing of PO_4^{3-} and Al^{3+} by a water-stable terbium-based metal-organic framework. *Spectrochim. Acta, Part A: Mol. and Biomol. Spectrosc.* **2021**, 247, 119084.
(111) Li, J. X.; Yu, B. Q.; Fan, L. H.; Wang, L.; Zhao, Y. C.; Sun, C. Y.; Li, W. J.; Chang, Z. D. A novel multifunctional Tb-MOF fluorescent probe displaying excellent abilities for highly selective detection of Fe^{3+}, $Cr_2O_7^{2-}$ and acetylacetone. *J. Solid State Chem.* **2022**, 306, 122782.
(112) Pang, J. J.; Du, R. H.; Lian, X.; Yao, Z. Q.; Xu, J.; Bu, X. H. Selective sensing of Cr^{VI} and Fe^{III} ions in aqueous solution by an exceptionally stable Tb^{III}-organic framework with an AIE-active ligand. *Chin. Chem. Lett.* **2021**, 32, 2443-2447.
(113) Li, B.; Dong, J. P.; Zhou, Z.; Wang, R.; Wang, L. Y.; Zang, S. Q. Robust lanthanide metal-organic frameworks with "all-in-one" multifunction: efficient gas adsorption and separation, tunable light emission and luminescence sensing. *J. Mater. Chem. C* **2021**, 9, 3429-3439.
(114) Zhao, Y. M.; Zhai, X.; Shao, L.; Li, L. L; Liu, Y. L.; Zhang, X. M.; Liu, J. H.; Meng, F. B.; Yu, F. An ultra-high quantum yield Tb-MOF with phenolic hydroxyl as the recognition group for a highly selective and sensitive detection of Fe^{3+}. *J. Mater. Chem. C* **2021**, 9, 15840-15847.
(115) Sun, Z.; Sun, J.; Xi, L.; Xie, J.; Wang, X. F.; Ma, Y.; Li, L. C. Two novel lanthanide metal-organic frameworks: selective luminescent sensing for nitrobenzene, Cu^{2+}, and MnO_4^-. *Cryst. Growth Des.* **2020**, 20, 5225-5234.
(116) Du, Y.; Yang, H. Y.; Liu, R. J.; Shao, C. Y.; Yang, L. R. A multi-responsive chemosensor for highly sensitive and selective detection of Fe^{3+}, Cu^{2+}, $Cr_2O_7^{2-}$ and nitrobenzene based on a luminescent lanthanide metal-organic framework. *Dalton Trans.* **2020**, 49, 13003-13016.
(117) Liao, W. M.; Wei, M. J.; Mo, J. T.; Fu, P. Y.; Fan, Y. N.; Pan, M.; Su, C. Y. Acidity and Cd^{2+} fluorescent sensing and selective CO_2 adsorption by a water-stable Eu-MOF. *Dalton Trans.* **2019**, 48, 4489-4494.
(118) Wang, X. Y.; Yao, X.; Huang, Q.; Li, Y. X.; An, G. H.; Li, G. M. Triple-wavelength-region luminescence sensing based on a color-tunable emitting lanthanide metal organic framework. *Anal. Chem.* **2018**, 90, 6675-6682.
(119) Wang, S. J.; Li, Q.; Xiu, G. L.; You, L. X.; Ding, F.; Deun, R. V.; Dragutan, L.; Dragutand, V.; Sun, Y. G. New Ln-MOFs based on mixed organic ligands: synthesis, structure and efficient luminescence sensing of the Hg^{2+} ions in aqueous solutions. *Dalton Trans.* **2021**, 50, 15612-15619.
(120) Wang, X. K.; Wang, Y. T.; Wang, X.; Lu, K. B.; Jiang, W. F.; Cui, P. P.; Hao, H. G.; Dai, F. N. Two series of Ln-MOFs by solvent induced self-assembly demonstrating the rapid selective sensing of Mg^{2+} and Fe^{3+} cations. *Dalton Trans.* **2020**, 49, 15473-15480.
(121) Wang, J. Y. S.; Yu, M. X.; Chen, L.; Li, Z. J.; Li, S. C.; Jiang, F. L.; Hong, M. C. Construction of a stable lanthanide metal-organic framework as a luminescent probe for rapid naked-eye recognition of Fe^{3+} and acetone. *Molecules* **2021**, 26, 1695.
(122) Li, J. L.; Xiao, Y.; Wang, L. Y.; Xing, Y. H.; Bai, F. Y.; Shi, Z. Oriented construction of the mixed-metal organic framework with triazine hexacarboxylic acid and fluorescence detection: Fe^{3+}, $Cr_2O_7^{2-}$ and TNP. *Polyhedron* **2022**, 214, 115648.
(123) Sun, T. C.; Fan, R. Q.; Xiao, R.; Xing, T. F.; Qin, M. Y.; Liu, Y. Q.; Hao, S. Chen, W.; Yang, Y. L. Anionic Ln-MOF with tunable emission for heavy metal ion capture and L-cysteine sensing in serum. *J. Mater. Chem. A* **2020**, 8, 5587-5594.
(124) Lin, Z. G.; Song, F. Q.; Wang, H.; Song, X. Q.; Yu, X. X.; Liu, W. S. The construction of a novel luminescent lanthanide framework for the selective sensing of Cu^{2+} and 4-nitrophenol in water. *Dalton Trans.* **2021**,

DOI: 10.14102/j.cnki.0254-5861.2022-0138

50, 1874-1886.
(125) Chen, Z.; Cai, Y. J.; Ma, Y. J.; Huang, L.; Zhao, Y. L.; Wang, L. Luminescent lanthanide complex sensor for Acac and Cd^{2+}. *Photochem. Photobiol.* **2021**, 97, 664-671.
(126) He, Q. Q.; Yao, S. L.; Zheng, T. F.; Xu, H.; Liu, S. J.; Chen, J. L.; Li, N.; Wen, H. R. A multi-responsive luminescent sensor based on a stable Eu(III) metal-organic framework for sensing Fe^{3+}, MnO_4^-, and $Cr_2O_7^{2-}$ in aqueous solutions. *CrystEngComm* **2022**, 24, 1041-1048.
(127) Li, X.; Tang, J. X.; Liu, H.; Gao, K.; Meng, X. R.; Wu, J.; Hou, H. W. A highly sensitive and recyclable Ln-MOF luminescent sensor for the efficient detection of Fe^{3+} and Cr^{VI} anions. *Chem. Asian J.* **2019**, 14, 3721-3727.
(128) Xu, X. Y.; Yan, B. A fluorescent wearable platform for sweat Cl^- analysis and logic smart-device fabrication based on color adjustable lanthanide MOFs. *J. Mater. Chem. C* **2018**, 6, 1863-1869.
(129) Dong, Z. P.; Zhao, F.; Zhang, L.; Liu, Z. L.; Wang, Y. Q. A white-light-emitting lanthanide metal-organic framework for luminescence turn-off sensing of MnO_4^- and turn-on sensing of folic acid and construction of a "turn-on plus" system. *New J. Chem.* **2020**, 44, 10239-10249.
(130) Duan, L. J.; Zhang, C. C.; Cen, P. P.; Jin, X. Y.; Liang, C.; Yang, J. H.; Liu, X. Y. Stable Ln-MOFs as multi-responsive photoluminescence sensors for the sensitive sensing of Fe^{3+}, $Cr_2O_7^{2-}$, and nitrofuran. *CrystEngComm* **2020**, 22, 1695-1704.
(131) Li, M. H.; Lv, S. L.; You, M. H.; Lin, M. L. Three-component D-A hybrid heterostructures with enhanced photochromic, photomodulated luminescence and selective anion-sensing properties. *Dalton Trans.* **2020**, 49, 13083-13089.
(132) Li, Z. D.; Zhan, Z. Y.; Jia, Y. J.; Li, Z.; Hu, M. A water-stable europium-MOF as a multifunctional luminescent sensor for some inorganic ions and dichloromethane molecule. *J. Ind. Eng. Chem.* **2021**, 97, 180-187.
(133) Li, B.; Zhou, J.; Bai, F. Y.; Xing, Y. H. Lanthanide-organic framework based on a 4,4-(9,9-dimethyl-9H-fluorene-2,7-diyl) dibenzoic acid: synthesis, structure and fluorescent sensing for a variety of cations and anions simultaneously. *Dyes and Pigments* **2020**, 172, 107862.
(134) Yuan, Z. D.; Hou, G. Z.; Han, L. J. A terbium-based MOF as fluorescent probe for the detection of malachite green, Fe^{3+} and MnO_4^-. *Z. Anorg. Allg. Chem.* **2021**, 647, 1-9.
(135) Li, Z. Y.; Cai, W. Y.; Yang, X. M.; Zhou, A. L.; Zhu, Y.; Wang, H.; Zhou, X.; Xiong, K. C.; Zhang, Q. F.; Gai, Y. L. Cationic metal-organic frameworks based on linear zwitterionic ligands for $Cr_2O_7^{2-}$ and ammonia sensing. *Cryst. Growth Des.* **2020**, 20, 3466-3473.
(136) Tan, G.; Jia, R. Q.; Wu, W. L.; Li, B.; Wang, L. Y. Highly pH-stable Ln-MOFs as sensitive and recyclable multifunctional materials: luminescent probe, tunable luminescent, and photocatalytic performance. *Cryst. Growth Des.* **2022**, 22, 323-333.
(137) Zhang, P. F.; Yang, G. P.; Li, G. P.; Yang, F.; Liu, W. N.; Li, J. Y.; Wang, Y. Y. Series of water-stable lanthanide metal-organic frameworks based on carboxylic acid imidazolium chloride: tunable luminescent emission and sensing. *Inorg. Chem.* **2019**, 58, 13969-13978.
(138) Ma, J. J.; Liu, W. S. Effective luminescence sensing of Fe^{3+}, $Cr_2O_7^{2-}$, MnO_4^- and 4-nitrophenol by lanthanide metal-organic frameworks with a new topology type. *Dalton Trans.* **2019**, 48, 12287-12295.
(139) Dong, Z. P.; Zhao, F.; Zhang, L.; Liu, Z. L.; Wang, Y. Q. A white-light-emitting lanthanide metal-organic framework for luminescence turn-off sensing of MnO_4^- and turn-on sensing of folic acid and construction of a "turn-on plus" system. *New J. Chem.* **2020**, 44, 10239-10249.
(140) Lu, Y. N.; Peng, J. L.; Zhou, X.; Wu, J. Z.; Ou, Y. C.; Cai, Y. P. Rapid naked-eye luminescence detection of carbonate ion through acetonitrile hydrolysis induced europium complexes. *CrystEngComm* **2018**, 20, 7574-7581.
(141) Min, H.; Han, Z. S.; Wang, M. M.; Li, Y. J.; Zhou, T. Z.; Shi, W.; Cheng, P. A water-stable terbium metal-organic framework as a highly sensitive fluorescent sensor for nitrite. *Inorg. Chem. Front.* **2020**, 7, 3379-3385.
(142) Li, B.; Zhou, J.; Bai, F. Y.; Xing, Y. H. Lanthanide-organic framework based on a 4,4-(9,9-dimethyl-9H-fluorene-2,7-diyl) dibenzoic acid: synthesis, structure and fluorescent sensing for a variety of cations and anions simultaneously. *Dyes and Pigments* **2020**, 172, 107862.
(143) Yu, M. K.; Yao, X.; Wang, X. Y.; Li, Y. X.; Li, G. M. White-light-emitting decoding sensing for eight frequently-used antibiotics based on a lanthanide metal-organic framework. *Polymers* **2019**, 11, 99.
(144) Yang, H. W.; Xu, P.; Wang, X. G.; Zhao, X. J.; Yang, E. C. A highly stable (4,8)-connected Tb-MOF exhibiting efficiently luminescent sensing towards nitroimidazole antibiotics. *Z. Anorg. Allg. Chem.* **2020**, 646, 23-29.
(145) Jiang, M. Y.; Yu, L.; Zhou, Y. C.; Jia, J.; Si, X. J.; Dong, W. W.; Tian, Z. F.; Zhao, J.; Li, D. S. A novel d-f heterometallic Cd^{II}-Eu^{III} metal-organic framework as a sensitive luminescent sensor for the dual detection of ronidazole and 4-nitrophenol. *Z. Anorg. Allg. Chem.* **2020**, 646, 268-274.
(146) Zhu, Q. Q.; He, H. H.; Yan, Y.; Yuan, J.; Lu, D. Q.; Zhang, D. Y.; Sun, F. X.; Zhu, G. S. An exceptionally stable Tb^{III}-based metal-organic framework for selectively and sensitively detecting antibiotics in aqueous solution. *Inorg. Chem.* **2019**, 58, 7746-7753.
(147) Guo, F.; Su, C. H.; Fan, Y. H.; Shi, W. B. An excellently stable Tb^{III}-organic framework with outstanding stability as a rapid, reversible, and multi-responsive luminescent sensor in water. *Dalton Trans.* **2019**, 48, 12910-12917.
(148) Wang, X. M.; Liu, C.; Wang, M.; Zhou, X. H.; You, Y. J.; Xiao, H. P. A selective fluorescence turn-on sensing coordination polymer for antibiotic aztreonam. *Chem. Commun.* **2022**, 58, 4667-4670
(149) Guo, Z. H.; Zhang, P. F.; Ma, L. L.; Deng, Y. X.; Yang, G. P.; Wang, Y. Y. Lanthanide-organic frameworks with uncoordinated Lewis base sites: tunable luminescence, antibiotic detection, and anticounterfeiting. *Inorg. Chem.* **2022**, 61, 6101-6109.
(150) Li, B.; Jiang, Y. Y.; Sun, Y. Y.; Wang, Y. J.; Han, M. L.; Wu, Y. P.; Ma, L. F.; Li, D. S. The highly selective detecting of antibiotics and support of noble metal catalysts by a multifunctional Eu-MOF. *Dalton Trans.* **2020**, 49, 14854-14862.
(151) Lei, M. Y.; Ge, F. Y.; Gao, X. J.; Shi, Z. Q.; Zheng, H. G. A water-stable Tb-MOF as a rapid, accurate, and highly sensitive ratiometric luminescent sensor for the discriminative sensing of antibiotics and D_2O in H_2O. *Inorg. Chem.* **2021**, 60, 10513-10521.
(152) Xue, Y. S.; Ding, J.; Sun, D. L.; Cheng, W. W.; Chen, X. R.; Huang, X. C.; Wang, J. 3D Ln-MOFs as multi-responsive luminescent probes for efficient sensing of Fe^{3+}, $Cr_2O_7^{2-}$, and antibiotics in aqueous solution. *CrystEngComm* **2021**, 23, 3838-3848.
(153) Fu, Y.; Zhang, R.; Lv, P.; Chen, F.; Xu, W. Eu-based metal-organic framework as a multi-responsive fluorescent sensor for efficient detecting $Cr_2O_7^{2-}$ and tetracycline hydrochloride. *J. Solid State Chem.* **2022**, 306, 122724.
(154) Wu, S. Y.; Zhu, M. C.; Zhang, Y.; Kosinova, M.; Fedin, V. P.; Gao, E. J. A water-stable lanthanide coordination polymer as multicenter platform

DOI: 10.14102/j.cnki.0254-5861.2022-0138

for ratiometric luminescent sensing antibiotics. *Chem. Eur. J.* **2020**, 26, 3137-3144.

(155) Yu, M. K.; Xie, Y.; Wang, X. Y.; Li, Y. X.; Li, G. M. Highly water-stable Dye@Ln-MOFs for sensitive and selective detection toward antibiotics in water. *ACS Appl. Mater. Interfaces* **2019**, 11, 21201-21210.

(156) Duan, L. J.; Zhang, C. C.; Cen, P. P.; Jin, X. Y.; Liang, C.; Yang J. H.; Liu, X. Y. Stable Ln-MOFs as multi-responsive photoluminescence sensors for the sensitive sensing of Fe^{3+}, $Cr_2O_7^{2-}$, and nitrofuran. *CrystEngComm* **2020**, 22, 1695-1704.

(157) Ren, K.; Wu, S. H.; Guo, X. F.; Wang, H. Lanthanide organic framework as a reversible luminescent sensor for sulfamethazine antibiotics. *Inorg. Chem.* **2019**, 58, 4223-4229.

(158) Ma, Y. X.; Zhu, M. C.; Zhang, Y.; Gao, E. J.; Wu, S, Y. A multiemissive lanthanide metal-organic framework for selective detection of L-tryptophan. *Inorg. Chim. Acta* **2022**, 537, 120928.

(159) Xia, T. F.; Wan, Y. T.; Li, Y. P.; Zhang, J. Highly stable lanthanide metal-organic framework as an internal calibrated luminescent sensor for glutamic acid, a neuropathy biomarker. *Inorg. Chem.* **2020**, 59, 8809-8817.

(160) Yang, D. D.; Lu, L. P.; Feng, S. S.; Zhu, M. L. First Ln-MOF as a trifunctional luminescent probe for the efficient sensing of aspartic acid, Fe^{3+} and DMSO. *Dalton Trans.* **2020**, 49, 7514-7524.

(161) Li, Y. G.; Hu, J. J.; Zhang, J. L.; Liu, S. J.; Peng, Y.; Wen, H. R. Lanthanide-based metal-organic framework materials as bifunctional fluorescence sensors toward acetylacetone and aspartic acid. *CrystEngComm* **2022**, 24, 2464-2471.

(162) Zhao, X. Y.; Wang, J.; Yang, Q. S.; Fu, D. L.; Jiang, D. K. A hydrostable samarium(III)-MOF sensor for the sensitive and selective detection of tryptophan based on a “dual antenna effect”. *Anal. Methods* **2021**, 13, 3994-4000.

(163) Wang, T. T.; Liu, J. Y.; Guo, R.; An, J. D.; Huo, J. Z.; Liu, Y. Y.; Shi, W.; Ding, B. Solvothermal preparation of a lanthanide metal-organic framework for highly sensitive discrimination of nitrofurantoin and L-tyrosine. *Molecules* **2021**, 26, 3673.

(164) Zhang, Y.; Lian, X.; Yan, B. A dual-functional intelligent logic detector based on new Ln-MOFs: first visual logical probe for the two-dimensional monitoring of pyrethroid biomarkers. *J. Mater. Chem. C* **2020**, 8, 3023-3028.

(165) Wang, X. Q.; Ma, X. H.; Feng, D. D.; Tang, J.; Wu, D.; Yang, J.; Jiao, J. J. Four novel lanthanide(III) metal-organic frameworks: tunable light emission and multiresponsive luminescence sensors for vitamin B6 and pesticides. *Cryst. Growth Des.* **2021**, 21, 2889-2897.

(166) Qu, X. L.; Yan, B. Zn(II)/Cd(II)-based metal-organic frameworks: crystal structures, Ln(III)-functionalized luminescence and chemical sensing of dichloroaniline as a pesticide biomarker. *J. Mater. Chem. C* **2020**, 8, 9427-9439.

(167) Zhang, W.; Xie, J.; Sui, Z. Y.; Xu, Z. J.; Wang, X. Z.; Lei, M.; Zhang, H. F.; Li, Z. Y.; Wang, Y. L.; Liu, W.; Du, W.; Wang, S. A. Ratiometric recognition of humidity by a europium-organic framework equipped with quasi-open metal site. *Sci. China Chem.* **2021**, 64, 1723-1729.

(168) Huizi-Rayo, U.; Zabala-Lekuona, A.; Terenzi, A.; Cruz, C. M.; Cuerva, J. M.; Rodrı´guez-Die´guez, A.; Garcı´a, J. A.; Seco, J. M.; Sebastian, E. S.; Ceped, J. Influence of thermally induced structural transformations on the magnetic and luminescence properties of tartrate-based chiral lanthanide organic-frameworks. *J. Mater. Chem. C* **2020**, 8, 8243-8256.

Received: May 26, 2022
Accepted: June 29, 2022
Published online: July 5, 2022
Published: October 31, 2022

Yan Yang received her Ph.D. degree in 2017 from Fujian Institute of Research on the Structure of Matter, Chinese Academy of Sciences, under the supervision of Prof. Maochun Hong. Subsequently, she started her teaching career at College of Chemistry and Chemical Engineering, Liaocheng University. Her research interests focus on the synthesis and practical applications of lanthanide metal-organic frameworks for chemical sensors.

Lian Chen graduated from Fudan University and received the B. Sc in 2002. From 2002 to 2007, she studied in Fujian Institute of Research on the Structure of Matter (FJIRSM), Chinese Academy of Sciences (CAS), and received her Ph.D. degree in 2007 under the supervision of Prof. Maochun Hong. Then, she joined the faculty at FJIRSM, CAS and was promoted to full research professor in 2018. Her research interests focus on the synthesis and property studies of organic-inorganic hybrid luminescent materials.

Shuting Xu received her B.Sc. degree from Liaocheng University in 2022. In the same year, she was admitted to the School of Chemistry and Chemical Engineering of Liaocheng University to pursue a M.Sc. degree under the supervision of Ph.D Yan Yang. Her research mainly focuses on the synthesis of lanthanide metal-organic frameworks and their applications for chemical sensors.

DOI: 10.14102/j.cnki.0254-5861.2022-0138

Yanli Gai received her Ph.D. degree from Fujian Institute Research on the Structural Chemistry, Chinese Academy of Sciences in 2014 under the supervision of Prof. Feilong Jiang and Prof. Maochun Hong. She joined the faculty at Jiangsu Normal University in 2015, and was promoted to Associate Professor in 2019. She worked as a visiting scholar in University of California at Riverside in 2017-2018. Her current research interests focus on metal-organic coordination polymers for chemical sensors, photo/chemochromism, and solid adsorbents for gas adsorption and separation.

Bo Zhang was born in Shandong, P. R. China. He received his Ph.D. degree in physical chemistry from Fujian Institute of Research on the Structure of Matter, Chinese Academy of Sciences, in 2017 under the supervision of Prof. Xiaoying Huang. In the same year, he joined the faculty at College of Chemistry and Chemical Engineering, Liaocheng University. His research interests focus on the design of energy and environment-related functional materials.

DOI: 10.14102/j.cnki.0254-5861.2022-0138